Vγ1^{+} γδ T cell-derived IL-4 initiates CD8 T cell immunity

Shirley Le[1], Declan Murphy[1], Shangyi Liu[1], Zhengyu Ge[1], Rose May[1], Anton Cozijnsen[2], Thomas Burn[1], Charlie Jennison[2], Annabell Bachem[1], Calvin Xu[1], Hui-Fern Koay[1], Jan Schröder[3], Stephanie Gras[4,5,6], Ian A. Cockburn[7], Sammy Bedoui[1], Laura K. Mackay[1], Geoffrey I McFadden[2], Daniel Fernandez-Ruiz[1,8], William R Heath[1#] and Lynette Beattie[1#*]

[1]Department of Microbiology and Immunology and The Peter Doherty Institute for Infection and Immunity, University of Melbourne, Parkville, Australia.

[2]School of Biosciences, University of Melbourne, Parkville, Australia.

[3]Computational Sciences Initiative, Department of Microbiology and Immunology and The Peter Doherty Institute for Infection and Immunity, University of Melbourne, Parkville, Australia.

[4]Infection and Immunity program, La Trobe Institute for Molecular Science (LIMS), La Trobe University, Bundoora, Australia.

[5]Department of Biochemistry and Chemistry, School of Agriculture, Biomedicine and environment, La Trobe University, Bundoora, Australia.

[6]Department of Biochemistry and Molecular Biology, Monash University, Clayton, Australia

[7]Division of Immunology and Infectious Disease, John Curtin School of Medical Research, Australian National University, Canberra, Australia.

[8]Current address, School of Biomedical Sciences, Faculty of Medicine & Health, and the UNSW RNA Institute, The University of New South Wales, Kensington, NSW 2052, Australia

[#]Senior authors

[*]Corresponding author and lead contact: lynette.beattie@unimelb.edu.au

Summary

Dendritic cells (DC) are pivotal for initiating adaptive immunity, a process triggered by the activation of DC via pathogen products or damage. Here, we describe an additional layer to this process, essential when pathogen-derived signals alone cannot directly achieve full DC activation. Immunisation with sporozoites from *Plasmodium* leads to CD8 T cell priming in a complex response that is initiated by conventional type 1 DC (cDC1). We unveil a pivotal initiating role for $V\gamma1^+$ γδ T cells, as they directly supply IL-4 to DC and CD8 T cells. IL-4 synergises with a CD4 T cell-derived CD40L signal to induce IL-12 production by cDC1. Both IL-12 and IL-4 then directly signal CD8 T cells, with synergy between these cytokines then driving enhanced IL-12 receptor expression and expansion of responding CD8 T cells. This study reveals a key role for $V\gamma l^+$ γδ T cells in initiating CD8 T cell immunity to *Plasmodium*. More broadly, it shows that responses to some pathogens require help from innate-like T cells to pass the initiation threshold and further amplify the response in a process underscored by IL-4 production.

Introduction

Priming of CD8 T cell responses involves a complex, multi-step process that relies on antigen presentation by DC that themselves must be sufficiently activated to provide all the necessary costimulatory signals. Classically, DC activation involves pattern recognition receptor (PRR) based detection of the pathogen itself, which induces costimulatory molecule expression and enhances MHC-II expression for antigen presentation to CD4 T cells[1]. These CD4 T cells, in turn, provide CD40L to the DC, allowing for DC licensing[2-4] and the production of pro-inflammatory cytokines such as IL-12, that contribute to T cell differentiation and expansion[5]. DC that are mature but not completely activated (or 'immunogenic') fail to produce pro-inflammatory cytokines[1], resulting in impaired T cell-mediated immunity[6]. The immune response to pathogens that induce strong pattern recognition receptor (PRR) signalling in DC, such as influenza viruses, are less dependent upon help from CD4 T cells to provide CD40L signalling for full DC immunogenicity[7]. Conversely, the responses to some pathogens, including herpes simplex virus[7] and other poor immunogens, are more dependent upon CD4 T cell help for full DC activation and licensing[8].

CD8 T cell responses to radiation attenuated *Plasmodium* sporozoites (RAS), are completely dependent upon help from CD4 T cells[9,10], placing *Plasmodium* sporozoites in the category of

67 'weak' pathogens. This response also depends upon CD40L signals[11], presumably from the
68 CD4 T cells, although this link has not been formally shown. RAS vaccination induces
69 sterilising protection in mice and humans[12,13] and is a powerful system to study the correlates
70 of protective immunity. Vaccination is most effective when the parasites are delivered
71 intravenously[14], likely due to the presence of antigen in the spleen where most conventional
72 αβ T cells are primed and undergo proliferative expansion[15]. Antigen presentation by type 1
73 conventional DC (cDC1) is essential for this process[15-17]. Once expanded, a proportion of the
74 CD8 T cells migrate to the liver and differentiate into liver resident memory T (T_{RM}) cells,
75 which are long-lived and provide protection against re-challenge with live parasites[18].
76 Interestingly, γδ T cells have been implicated in the development of this response[19], though just
77 how these cells contribute is unclear.
78
79 γδ T cells are innate sensors[20] and are often the first responders to infection, stress, or
80 damage[20,21]. They are of particular interest in the field of immunotherapy as, unlike αβ T cells,
81 γδ T cells are not restricted by human leukocyte antigen (HLA) haplotype[22]. The specific
82 antigens or molecules that γδ T cells recognise are still largely unknown but in addition to
83 recognising a small number of pathogen antigens[23], γδ T cells also recognise signs of altered
84 self, induced via damage or stress[24], or altered metabolism driven by infection, autoimmunity
85 or cancer[25]. Once activated, γδ T cells exert diverse effector mechanisms including the rapid
86 release of various cytokines including interleukin (IL-) 17[26], TNF, IFN-γ and IL-4[27,28]. In mice,
87 there are 6 populations of γδ T cells segregated via expression on $V\gamma1^+$, $V\gamma2^+$, $V\gamma4^+$, $V\gamma5^+$, $V\gamma6^+$
88 and $V\gamma7^+$ respectively (Heilig and Tonegewa nomenclature[29]). Of these, $V\gamma1^+$, and $V\gamma4^+$
89 populations are found in lymphoid tissues including the spleen. In humans, the predominant γδ
90 T cell subsets express either $V\delta1^+$, $V\delta2^+$ or $V\delta3^+$, with the majority of $V\delta2^+$ cells preferentially
91 pairing with Vγ9[30]. Vδ2Vγ9 γδ T cells are the most abundant γδ T cell population in human
92 peripheral blood and known to react to phosphoantigens[31]. Strong correlations between γδ T
93 cell functions and the generation of protective immunity following RAS vaccination[19,32,33] have
94 been established. RAS vaccination in malaria-naïve adults leads to a dose-dependent expansion
95 of $V\delta2^+$ T cells, and this is linked to the priming of *P. falciparum* sporozoite (Pf-SPZ)-specific
96 T cells and disease protection[32,34]. $V\delta2^+$ T cells are more abundant in Pf -SPZ vaccinated adults
97 that remain uninfected during follow-up[35]. However, the molecular pathways driving these

98 associations, the specific γδ T cell populations involved, and the molecular signals they
99 contribute to protective immunity remain unclear.
100
101 Here, we show that the Vγ1^{+} subset of γδ T cells drives an activation program in cDC1 that
102 initiates the CD8 T cell response to liver stage malaria parasites via IL-4 production, which
103 enhances production of and sensitivity to IL-12. Our data have implications for our
104 understanding of how CD8 T cell responses to poor immunogens can be strengthened early in
105 the priming phase and reveal a role for Vγ1^{+} γδ T cells and IL-4 in enhancing CD8 T cell
106 responses.
107
108 **Results**
109 **γδ T cells are essential for RAS-induced liver T_{RM} cell generation**
110 Immunity to RAS vaccination is impaired in γδ T cell-deficient mice, due to impaired
111 generation of *Plasmodium*-specific memory T cells in the liver[19]. Liver T_{RM} cells are the major
112 population that mediate protection against liver stage infection[18], but previous studies in γδ T
113 cell deficient mice only looked generally at the CD8 memory T cell response without
114 quantifying specific subsets of memory T cells. Therefore, we specifically assessed whether
115 induction of liver T_{RM} cells was impaired in γδ T cell-deficient mice. We vaccinated C57BL/6
116 (B6) or γδ T cell deficient *Tcrd*$^{-/-}$ (δ$^{-/-}$) mice with RAS and quantitated memory T cell responses
117 in the liver. Examination of the liver for memory T cells specific for the *P. berghei*-derived
118 RPL6 protein[36] with the peptide sequence NVFDFNNL (PbRPL6$_{120-127}$) (**Figure 1A, B and**
119 **Supplementary Figure 1A and B**) and TRAP[37] (**Figure 1C, D and Supplementary Figure**
120 **1A and B**), 35 days post-vaccination, revealed poor generation of memory T cells in the liver
121 in the absence of γδ T cells, with a preferential loss of liver T_{RM} cells (**Figure 1B and D**).
122 Fewer RPL6- and TRAP-specific memory T cells were also seen in the spleen between WT
123 and δ$^{-/-}$ mice at this time point (**Supplementary Figure 1C-F**). These data expand upon
124 previous observations[19] to show a specific and major defect in *Plasmodium*-specific liver T_{RM}
125 cell generation in the absence of γδ T cells. Consistent with this observation, RAS-vaccinated
126 δ$^{-/-}$ mice challenged with *P. berghei* sporozoites (**Figure 1E**) were unable to control infection,
127 as indicated by patent parasitemia within 7 days (**Figure 1F**). γδ T cells are therefore crucial
128 for RAS vaccination-induced generation of protective liver T_{RM} cells.
129

130 We next assessed whether γδ T cells were also required for other forms of sporozoite-based
131 vaccination, including genetically attenuated parasite (GAP) vaccination, which induces a
132 stronger response to a broader range of parasite antigens than RAS vaccination[38]. B6 or $\delta^{-/-}$
133 mice were vaccinated with a *P. berghei* gene deletion mutant lacking the *mei2* gene (PbΔ*mei2*).
134 These parasites do not differentiate into blood stage parasites but persist in the liver late into
135 the liver stage[39]. B6 mice vaccinated with a single dose of PbΔ*mei2* generated memory T cells
136 against RPL6[40] (**Figure 1G and H and Supplementary Figure 1A, B, G and H**) but these
137 responses were impaired in $\delta^{-/-}$ mice. Thus, the γδ T cell-dependence of the liver CD8 memory
138 T_{RM} cell response extended to GAP.
139
140 To determine if these findings extend to TCR transgenic T cells, which are a useful tool to
141 dissect early events in priming, we utilized cells from the MHC-I restricted *P. berghei*-specific
142 TCR transgenic mouse line termed PbT-I[15 36]. PbT-I T cells were adoptively transferred into
143 B6 or $\delta^{-/-}$ mice, the mice injected with RAS, and the PbT-I T cell number and phenotype
144 assessed 3 weeks later. Memory PbT-I cells were dramatically reduced in $\delta^{-/-}$ mice compared
145 to B6 mice (**Figure 1I and Supplementary Figure 1I**) with a specific defect in the number of
146 T_{RM} cells (**Figure 1J and Supplementary Figure 1J**). These defects indicate PbT-I cells
147 behave much like the endogenous repertoire (**Figure 1A-D**).
148
149 **γδ T cells affect early expansion of CD8 and CD4 T cells**
150 The T cell response to RAS is initiated largely in the spleen with priming and expansion
151 occurring in this site, followed by recirculation and resultant rapid accumulation of activated
152 T cells in the liver 3 days later[15]. To ascertain whether the defect in $\delta^{-/-}$ mice occurred early in
153 the splenic priming response, naïve PbT-I T cells were transferred into B6 and $\delta^{-/-}$ mice and
154 their number assessed 6 days later in the spleen (**Figure 2A**) and the liver (**Figure 2B**). This
155 revealed a defect in the accumulation of PbT-I T cells in each site, likely due to an initial failure
156 to respond in the spleen, which would impair accumulation in this site and prevent their
157 migration and accumulation in the liver. These findings indicate that a defect in priming in the
158 spleen underlies lack of a memory response in the liver.
159
160 Of note, the poor initial response in $\delta^{-/-}$ mice only extended to vaccination with the sporozoite
161 form of this parasite as responses to blood-stage parasites (irradiated infected red blood cells)

were unaffected (**Supplementary Figure 2A**), indicating that priming with this form of the parasite is not dependent on help from γδ T cells.

RAS-induced expansion of CD8 T cells is CD4 T cell dependent[9,10]. Therefore, we assessed whether CD4 T cell accumulation in the spleen in response to RAS immunisation was also γδ T cell dependent. Here we utilized PbT-II cells[41] from the MHC-II restricted P. *berghei*-specific TCR transgenic line[42]. These CD4 T cells were co-transferred with PbT-I cells into B6 or $\delta^{-/-}$ mice that were then vaccinated with RAS and responses assessed on day 6 (**Figure 2C**). The accumulation of both PbT-I (**Figure 2D**) and PbT-II T cells (**Figure 2E**) was lower in the spleen of $\delta^{-/-}$ mice, showing that γδ T cells are required for the accumulation of both CD4 and CD8 T cells. This also indicated that the addition of large numbers of naïve antigen-specific CD4 T cells could not rescue the response of CD8 PbT-I T cells when γδ T cells were absent.

Splenic Vγ1$^+$ γδ T cells are activated within 24 hours of RAS vaccination

To ascertain when γδ T cells affect CD4 and CD8 T cell responses, we utilised the pan-TCRδ blocking antibody (clone GL3)[43] to block γδ T cell function at the time of, or 24 hr after RAS vaccination (**Figure 2F**). PbT-I T cell accumulation was then examined in the spleen 6 days later. Blocking γδ T cell function at the time of RAS vaccination resulted in a defect in PbT-I cell accumulation comparable to that previously observed in $\delta^{-/-}$ mice (**Figure 2G**) (14.6 fold-decrease in PbT-I cell numbers in GL3 treated mice compared to isotype controls). In contrast, blocking γδ T cell function from 24 hr post-RAS injection had a much milder effect (**Figure 2G**) (5.16 fold-decrease of GL3 treated mice compared to isotype controls). These data suggest that the first 24 hr is the crucial window of γδ T cell activation and that they act early in the T cell priming phase.

Knowing that the first 24 hours were critical, we next examined early γδ T cell activation. Splenic γδ T cells were split into the two major populations found in murine spleen, Vγ1$^+$ or Vγ1$^-$ populations (**Supplementary Figure 2B**). Up-regulation of the canonical T cell activation markers CD69, CD25 and CD11a was seen at 24 hours in the Vγ1$^+$ γδ T cell population, indicating that these cells were activated at this timepoint (**Figure 2H and I and Supplementary Figure 2C**). Attempts to detect cytokine secretion within this population of cells were unsuccessful, likely due to the very small magnitude of the response.

195 To investigate if the activated Vγ1$^+$ γδ T cells were having a functional effect on the CD8 T cell
196 response, we blocked Vγ1 function through the administration of a Vγ1 blocking antibody
197 (clone 2.11)[44] (**Figure 2J**) and examined PbT-I T cell accumulation in the spleen 6 days after
198 RAS vaccination. Blockade of the Vγ1$^+$ population had the same effect as blockade of the entire
199 γδ T cell population (αGL3) (**Figure 2K**). Therefore, Vγ1$^+$ γδ T cells are activated in response
200 to RAS vaccination and have a functional impact on the accumulation of CD8 T cells.
201
202 **Antigen presentation of *Plasmodium*-derived peptides is intact in the absence of γδ T cells**
203 Due to the very early timing of γδ T cell activation, and the effect of γδ T cells on CD8 T cell
204 accumulation in the spleen, we hypothesised that the Vγ1$^+$ γδ T cells may impact the ability of
205 cDC1 to present antigen to CD8 T cells in response to RAS vaccination. To investigate this
206 possibility, we examined initial up-regulation of CD69 within the antigen-specific CD8 T cell
207 population. It was not possible to use PbT-I T cells for this assay, as T cell transfer induces
208 spontaneous up-regulation of CD69 on PbT-I T cells for reasons yet to be determined. We
209 therefore used OT-I T cells, which do not exhibit spontaneous CD69 upregulation upon
210 transfer, allowing for sensitive detection of antigen presentation to these cells. This system also
211 required the use of SIINFEKL expressing *Plasmodium* parasites, termed CS5M, which express
212 the cognate antigen for OT-I T cells[45].
213
214 OT-I T cells were labelled with cell trace violet (CTV) and adoptively transferred into B6 or δ$^-$
215 $^{/-}$ mice that were subsequently injected with irradiated CS5M sporozoites (CS5M-RAS). At
216 various times between day 1 and 6, we examined CTV dilution and CD69 expression on OT-I
217 T cells isolated from several tissues (spleen, liver draining lymph nodes (LdLN), liver, and a
218 control LN). In the spleen, equal proportions (**Figure 3A and B**) and numbers (**Figure 3C**) of
219 OT-I T cells up-regulated cell surface expression of CD69 in B6 and δ$^{-/-}$ mice on days 1 and 2
220 post-vaccination. Similar proportions and numbers of activated OT-I T cells were also observed
221 in the LdLN, liver, and control LN on days 1 and 2 (**Supplementary Figure 3**). However, by
222 day 6, significantly more OT-I T cells were present in B6 spleens (**Figure 3D**), liver and LdLN
223 (**Supplementary Figure 3**), recapitulating observations with endogenous RPL6-specific and
224 PbT-I T cells. The very early activation of OT-I cells on days 1 and 2 indicated access to antigen
225 even when γδ T cells were absent, showing that antigen presentation was intact in the absence
226 of γδ T cells, but that the responding T cells were not provided with signals required for
227 extended expansion and/or survival. As antigen presentation appeared to be intact, this

228 observation strongly suggested a lack of co-stimulation or cytokines in the T cell priming
229 process, raising the intriguing possibility that γδ T cells trigger upregulation of co-stimulation-
230 like signals on cDC1.
231
232 **γδ T cells are not required to supply the CD40L signal to cDC1**
233 As a deficiency in co-stimulation was implicated, we hypothesised that γδ T cells may provide
234 CD40L for signalling CD40 on cDC1, a signal known to be essential in the response to RAS[11].
235 To investigate this possibility, PbT-I T cells were transferred into control groups of WT and δ^{-}
236 $^{/-}$ mice as well as two groups of *Cd40l*$^{-/-}$ mice. CD8 T cell expansion is dependent on help from
237 CD4 T cells in the RAS model[9,10], and these CD4 T cells were previously presumed to provide
238 the CD40L signal. To test whether CD4 T cells can provide the essential CD40L signal, one
239 group of *Cd40l*$^{-/-}$ mice were also given CD40L sufficient PbT-II cells (**Figure 3E**). PbT-I T cell
240 accumulation in the spleen 6 days after RAS injection was severely diminished in *Cd40l*$^{-/-}$ mice
241 (**Figure 3F**), confirming that CD8 T cell accumulation in this model is dependent on CD40L
242 signalling. Addition of CD40L sufficient PbT-II T cells, however, rescued the PbT-I T cell
243 response, even though γδ T cells lacked expression of CD40L in these mice (**Figure 3F**). This
244 finding supports the view that CD4 T cells can provide the CD40L signalling required for the
245 response to RAS and suggests that γδ T cells are not required to provide this co-stimulatory
246 function. Furthermore, rescue by CD40L sufficient PbT-II cells shows that this signal is
247 normally provided by CD4 T cells but is insufficient to ensure an appropriate CD8 T cell
248 response if γδ T cells are absent (**Figure 3F and G**).
249
250 **IL-4 is required for the CD8 T cell response to RAS vaccination**
251 As γδ T cells were not the crucial source of CD40-CD40L signals, we rationalised that they
252 may be providing 'signal 3' for differentiation and expansion after initial T cell activation, i.e.
253 a cytokine signal. Previous studies suggested IL-4 is a crucial factor in the generation of
254 memory CD8 T cells in the liver following RAS vaccination[46,47]. Given that splenic Vγ1^{+} γδ T
255 cells have been reported to secrete IL-4[28], we next investigated the role of IL-4 in the PbT-I T
256 cell response either via transfer into *Il4*$^{-/-}$ hosts (**Figure 4A and B**) or antibody-mediated
257 blockade (S**upplementary Figure 4A and B**). These data showed that IL-4 was crucial for the
258 accumulation of PbT-I T cells in the spleen in response to RAS vaccination, mirroring the effect
259 of γδ T cell deficiency.
260

261 To further investigate if, as previously reported, CD4 T cells are the relevant source of IL-4[46],
262 we transferred IL-4 sufficient PbT-I T cells with, or without, IL-4 sufficient PbT-II T cells into
263 B6 or *Il4*$^{-/-}$ mice and measured T cell accumulation as the output. As demonstrated above, the
264 accumulation of PbT-I T cells was substantially lower in the *Il4*$^{-/-}$ mice when compared to the
265 B6 controls (**Figure 4C**), but this remained the case even in the presence of antigen-specific
266 CD4 T cells that could make IL-4. In contrast, antigen-specific CD4 PbT-II T cells expanded
267 in the spleen in both B6 and *Il4*$^{-/-}$ mice (**Figure 4D**) demonstrating two phenomena; 1) CD4 T
268 cell accumulation in the spleen in response to RAS vaccination is not IL-4 dependent, as equal
269 accumulation was seen in B6 and *Il4*$^{-/-}$ mice and 2) IL-4 sufficient CD4 T cells did not rescue
270 the antigen-specific CD8 T cell response. CD4 T cells, therefore, are not the crucial source of
271 IL-4 for CD8 T cell accumulation following RAS vaccination.
272
273 **γδ T cells are the source of IL-4**
274 To determine if γδ T cells provide IL-4 in response to RAS vaccination, we used a mixed bone
275 marrow (BM) chimera approach. As not all γδ T cells are reconstituted from the BM[48,49], we
276 first confirmed that the Vγ1^{+} γδ T cell population, important for T cell accumulation in response
277 to RAS, was replenished from the BM. Cohorts of lethally irradiated B6 or δ$^{-/-}$ mice received
278 BM cells from congenic Ly5.1 or δ$^{-/-}$ mice according to the scheme described in **Figure 4E**.
279 The endogenous γδ T cell populations, stratified into Vγ1^{-} and Vγ1^{+} subpopulations, were
280 reconstituted from the BM (**Figure 4F**), as was the accumulation of PbT-I T cells in Ly5.1→B6
281 but not in δ$^{-/-}$→B6 chimeras in response to RAS vaccination, mirroring outcomes for non-
282 irradiated WT or δ$^{-/-}$ mice, respectively (**Figure 4G**).
283
284 To investigate if γδ T cells are the crucial source of IL-4 in response to RAS vaccination, we
285 made six groups of mixed BM chimeras (**Figure 5H**). The groups were: 1. B6→B6, 2. *Il4*$^{-/-}$
286 →B6, 3. B6→*Il4*$^{-/-}$, 4. B6+δ$^{-/-}$→B6, 5. *Il4*$^{-/-}$ +δ$^{-/-}$→B6, and 6. δ$^{-/-}$→B6. For the mixed BM
287 chimeras, a 50:50 ratio of BM was used. Eight weeks after reconstitution, the γδ T cell
288 compartment was reconstituted as expected (**Figure 5I**). PbT-I T cells were transferred into
289 chimeras before vaccination with RAS and subsequent assessment of CD8 T cell responses 6
290 days later (**Figure 4J**). Comparison of PbT-I accumulation in the spleen of B6→ B6 (group 1)
291 versus *Il4*$^{-/-}$ → B6 (group 2) chimeras showed impaired PbT-I T cell accumulation in the *Il4*$^{-/-}$
292 → B6 BM chimeras, recapitulating findings observed in IL-4 knockout mice (**Figure 4J**).

293 Comparison of *Il4*$^{-/-}$ → B6 (group 2) and B6 → *Il4*$^{-/-}$ (group 3) chimeras confirmed that the IL-
294 4 producing population was of BM origin, as responses in the B6 → *Il4*$^{-/-}$ chimers showed
295 improved accumulation, which was comparable to wild-type B6→ B6 (group 1) chimeras.
296 Crucially, PbT-I accumulation in the spleen of *Il4*$^{-/-}$ +δ$^{-/-}$→B6 chimeras (group 5) was
297 significantly lower than that observed in the B6+δ$^{-/-}$→B6 chimeras (group 4) (**Figure 4J**). The
298 difference between these groups was that the B6+δ$^{-/-}$→B6 chimeras contained γδ T cells that
299 could produce IL-4, whereas the *Il4*$^{-/-}$+δ$^{-/-}$→B6 chimeras lacked these cells. These data strongly
300 suggest that γδ T cells are the essential source of IL-4 for the development of an effective CD8
301 T cell response to RAS vaccination.
302
303 To further confirm that γδ T cells are the crucial source of IL-4, we reconstituted δ$^{-/-}$ mice with
304 splenic γδ T cells from either WT *or Il4*$^{-/-}$ donors and tested whether these cells could rescue
305 the PbT-I T cell accumulation following RAS vaccination. TCRδ-deficient mice received either
306 splenic γδ T cells or no γδ T cell transfer (**Figure 4K**). Six days after RAS vaccination (8 days
307 after γδ T cell transfer), γδ T cells were recovered from the spleens of the groups that received
308 the γδ T cell transfer (**Figure 4L**). As hypothesised, B6-derived but not *Il4*$^{-/-}$-derived γδ T cells
309 supported PbT-I T cell accumulation in the spleen, confirming that these cells provide IL-4 in
310 this vaccination setting (**Figure 4M**).
311
312 **CD8 T cells respond directly to IL-4**
313 To investigate the target of IL-4 produced in response to RAS vaccination, we asked if IL-4
314 acts directly on the responding CD8 T cells. To address this question, we established a CRISPR-
315 Cas9 system to knock the IL-4Rα gene (*Il4ra*) out in T cells. Purified naïve PbT-I and/or PbT-
316 II T cells had *Il4ra* (or *Cd19* as a control) knocked out prior to transfer and immunisation with
317 RAS (**Figure 5A**). Six days after vaccination, we confirmed efficient deletion of IL-4Rα
318 expression on PbT-I (**Figure 5B**) and PbT-II T cells (**Figure 5C**) via flow cytometry.
319 Comparison of the number of PbT-I T cells 6 days after RAS vaccination showed that direct
320 IL-4Rα signalling in PbT-I T cells was important for PbT-I T cell accumulation in the spleen
321 with lower numbers of PbT-I T cells observed in the sg*Il4ra* PbT-I T cell group than in the
322 sg*Cd19* controls (**Figure 5D**). Deleting *Il4ra* in PbT-II T cells had no effect on the number of
323 PbT-II T cells recovered (**Figure 5D**), indicating that CD4 T cells do not need to receive IL-

324 4Rα signals to accumulate in the spleen following RAS vaccination. As expected, neither PbT-
325 I nor PbT-II cells responded in the α-GL3 treated groups (**Figure 5C and D**).
326
327 **IL-4 signalling in cDC1 is also required for optimal CD8 priming**
328 PbT-I T cells lacking the IL-4R still retained a modest capability to accumulate when compared
329 to a complete failure in the absence of γδ T cells (**Figure 5C**), or IL-4 itself (**Figure 4B**). This
330 suggested that IL-4 has an additional activity that contributes to CD8 T cell accumulation. To
331 investigate whether this involved effects on cDC1 responsible for priming[15], we developed an
332 *in vivo* model for cDC1 manipulation. To establish this model, donor cDC1 were expanded *in*
333 *vivo* in B6 mice[50] prior to enrichment and adoptive transfer into *Batf3*$^{-/-}$ mice for replenishment
334 of the cDC1 pool (**Figure 5F**). The following day, mice were vaccinated with RAS and the
335 accumulation of PbT-I T cells assessed 6 days later. Accumulation of PbT-I T cells in the
336 reconstituted *Batf3*$^{-/-}$ mice was significantly higher when compared to the group that were not
337 administered DC (**Figure 5G**), demonstrating functional reconstitution of the cDC1 pool. We
338 then used this system to determine if the direct signalling of cDC1 by IL-4 was important for
339 the CD8 T cell response to RAS by knocking out IL-4Rα expression in cDC1. cDC1 were
340 expanded and then isolated, purified and electroporated with either sg*Cd19* or sg*Il4ra* then
341 transferred into *Batf3*$^{-/-}$ mice. Two days later, PbT-I T cells were transferred, and the mice
342 vaccinated with RAS for assessment of PbT-I T cell numbers 6 days later. Numbers of cDC1
343 recovered 6 days post-RAS vaccination were equivalent between the mice that received control
344 (*sgCd19*) or *Il4ra* knockout DC demonstrating equivalent reconstitution (**Figure 5H and**
345 **Supplementary Figure 5A**). However, the number of PbT-I cells that accumulated in the
346 spleens of mice that received control (sg*Cd19*) DC was significantly higher than the numbers
347 in mice that received IL-4Rα-deficient (sg*Il4ra*) DC (**Figure 5I**). Collectively, these
348 experiments demonstrate that IL-4 acts directly on DC and CD8 T cells for optimal CD8
349 expansion in the context of RAS vaccination (**Figure 5J**).
350
351 **CD40 and IL-4 synergise to drive IL-12 production by DC**
352 To identify the molecules induced by IL-4 in cDC1 that may contribute to the response to RAS
353 vaccination, cDC1 gene expression was assessed *in vitro* following stimulation with IL-4 and
354 αCD40. Expanded cDC1 were sort-purified and then cultured in each condition before
355 isolation of RNA at 4 hours, a timepoint previously shown to be optimal for assessment of gene

356 expression in cDC[51]. Sorted cDC1 were assessed after exposure to the following conditions:
357 media alone, αCD40, IL-4, and αCD40+IL-4 (**Figure 6A**).
358
359 Analysis of sequenced RNA revealed a marked transcriptomic shift in the presence of IL-4 that
360 was augmented by the addition of αCD40 (**Figure 6B**). Specifically, there were 841 up-
361 regulated and 762 down-regulated genes in response to CD40+IL-4 when compared to media
362 alone (**Figure 6B**). *Il12a*, was the most upregulated gene when comparing media with
363 CD40+IL-4 (LFC 11.17, FDR $1.5x10^{-59}$) and the second most upregulated gene when
364 comparing CD40+IL-4 with CD40 alone (LFC 11.69, FDR $1.48x10^{-52}$) (**Figure 6C and D**).
365 This gene encodes the p35 subunit of IL-12 and when combined with the p40 subunit (which
366 is constitutively expressed by cDC1), makes bioactive IL-12, a key stimulator of CD8 T cells.
367 As it was only weakly upregulated in cDC1 exposed to IL-4 alone, efficient upregulation of
368 *Il12a* also appeared dependent on the combination of both CD40 and IL-4 (**Figure 6D**).
369
370 To determine the contribution of bioactive IL-12 *in vivo* in the context of RAS vaccination,
371 PbT-I T cell accumulation was assessed after IL-12 blockade. Mice were given PbT-I T cells
372 and then the next day immunized with RAS and left untreated or given blocking antibody
373 against the IL-12p40 subunit (**Figure 6E**). Assessment of PbT-I accumulation on day 6 showed
374 significant impairment when IL-12 was blocked (**Figure 6F**). This supports a model where
375 CD40 signalling synergises with IL-4 in cDC1 to induce IL-12 that is crucial for the
376 accumulation of CD8 T cells in response to RAS vaccination (**Figure 6G**).
377
378 **IL-4 and IL-12 synergise to enhance CD8 T cell expansion**
379 IL-4 and IL-12 were both essential for the enhanced accumulation of CD8 T cells in response
380 to RAS vaccination. This led us to investigate whether these cytokines work synergistically to
381 promote CD8 T cell expansion. To isolate the effects of the cytokines, we first examined the
382 impact of IL-4 and IL-12 on CD8 T cell expansion *in vitro*.
383
384 PbT-I T cells were activated by peptide coated antigen presenting cells in the presence of; no
385 added cytokine, IL-4, IL-12, or IL-12 and IL-4, and the number of cells retrieved from the
386 cultures enumerated on day 4 and day 6. Limited cell growth was observed in the absence of
387 exogenous cytokine (**Figure 7A**) and addition of either IL-4 or IL-12 only modestly impacted
388 the number of cells recovered between day 4 and day 6 (**Figure 7B and C).** In contrast, addition

389 of both IL-4 and IL-12 resulted in significantly higher cell recovery from the culture on day 6
390 (**Figure 7D**). These data suggested that the combination of IL-4 and IL-12 act synergistically
391 in increasing the T cell response *in vitro*.
392
393 To explore whether the synergy between IL-4 and IL-12 was mediated by changes in cytokine
394 sensitivity resulting from alterations in receptor expression, we assessed IL-4R and IL-12R
395 expression on T cells at day 4 of culture. Addition of both IL-4 and IL-12 induced a small but
396 significant increase in the expression of IL-4R on the T cells when compared to addition of IL-
397 4 alone (**Figure 7E**). In contrast, the addition of both IL-4 and IL-12 resulted in a substantial
398 increase in the expression of IL-12R over either cytokine alone (**Figure 7F**). These data
399 suggested that the combination of IL-4 and IL-12 amplifies the sensitivity of CD8 T cells to
400 IL-12 signalling through increased expression of IL-12R, thereby enhancing the CD8 T cell
401 response. Further, *in vitro* activated OT-I T cells stimulated with IL-4 and IL-12 were
402 maintained in greater numbers when transferred into mice (**Figure 7G**).
403
404 **Combined IL-4 and IL-12 signals control the development of liver T_{RM} in response to**
405 **RAS vaccination.**
406 The phenotype originally observed in γδ T cell knockout mice was a deficiency of liver T_{RM}
407 cells after RAS vaccination, resulting in reduced protection against challenge infection. Our
408 findings demonstrated that γδ T cells produced IL-4 in response to RAS vaccination, which
409 enhanced CD40-mediated activation of cDC1 and boosted IL-12 production. Additionally,
410 combined IL-4 and IL-12 signalling in activated T cells increased the expression of IL-12R and
411 therefore sensitivity to IL-12, promoting their expansion. To confirm that removal of both IL-
412 4 and IL-12 *in vivo* would recapitulate the lack of γδ T cells and therefore inhibit the formation
413 of liver resident memory T cells, we blocked IL-4 or IL-12, or both, in the context of RAS
414 vaccination, and then examined T_{RM} numbers in the liver 35 days later (**Figure 7H-J**). PbT-I
415 cells were transferred into WT mice and IL-4 and/or IL-12 blocking antibodies administered
416 before and after RAS vaccination (**Figure 7H**). Enumeration of the number of liver T_{RM} cells
417 present showed that IL-4 had a dominant effect on liver T_{RM} formation, but blockade of both
418 cytokines phenocopied blockade of γδ T cells (with αGL3 Ab) in the liver (**Figure 7K and L)**
419 and in the spleen (**Figure 7I and J**). These data showed that γδ T cells drive the response to
420 RAS via delivery of IL-4 to DC, which in turn drives IL-12 production. The γδ T cell derived

421 IL-4 and DC-derived IL-12 then synergise to enhance the expansion of CD8 T cells (**Figure**
422 **7M**), a proportion of which will differentiate into protective liver T_{RM} cells.
423
424 **Discussion**
425 For full immunogenicity, DC must be effectively activated, either via strong PRR signalling or
426 through CD4 T cell help via CD40L[1]. Here, we showed that the priming of CD8 T cells to
427 *Plasmodium* sporozoite antigens depends on an additional layer of DC activation via IL-4,
428 which is produced by γδ T cells. Here, IL-4 has a dual role: 1) when synergised with CD40
429 signals in DC, it promotes enhanced production of bioactive IL-12 and 2) by directly signalling
430 CD8 T cells to increase IL-12R, it increases their sensitivity to IL-12 and thereby promotes
431 expansion. In this vaccination setting, IL-4 is produced by $V\gamma1^+$ γδ T cells in the spleen, which
432 become activated within the first 24 hours of injection of sporozoites.
433
434 The absolute requirement for γδ T cells in RAS vaccination in mice[19] and in humans[19,32,34,52]
435 suggests that although *Plasmodium* sporozoites are reported to trigger toll like receptor 2
436 signalling[53], this stimulation is not sufficient to push DC over a required activation threshold
437 and that an additional IL-4 signal in combination with CD40 is required. Our findings likely
438 extend beyond the context of RAS vaccination, applicable to other scenarios involving poor
439 immunogens. In such cases, the sensing of infection or cellular damage by innate or innate-like
440 cells may trigger IL-4 production, thereby enabling DC to effectively prime protective immune
441 responses. One such innate-like T cell population are invariant natural killer T (NKT) cells,
442 which are known to produce IL-4 in response to lipid ligands[54] but the need for NKT cell-
443 derived cytokines on top of CD4 T cell help in a four-cell paradigm, as we have shown here
444 for γδ T cells, has not been described.
445
446 In mice, γδ T cell-derived IL-17[55] and IFN-γ[56], induced by liver-stage parasites have been
447 shown to play important roles in the pathology of *Plasmodium* blood stage infection. Moreover,
448 we have shown that the initiation of the CD4 response to liver stage parasites is also dependent
449 on a factor provided by γδ T cells but have not yet identified what that factor is. These concepts
450 highlight that γδ T cells play a varied and substantial role in malaria disease.
451
452 Previous studies that described a role for γδ T cells in RAS vaccination proposed that a
453 population of CD8 DC that accumulated in the liver of RAS vaccinated mice when γδ T cells

were present also correlated with the generation of hepatic CD8 T cell memory[19]. Although we have not directly investigated or ruled out a role for these hepatic DC in the memory component of the response to RAS, our data show that splenic cDC1 collaborate with γδ T cells to drive efficient priming of splenic CD8 T cells. It is possible that the inflammation induced by the combination of IL-4 and IL-12 observed when γδ T cells are present also leads to inflammation in the liver and the accumulation of CD8 cDC, commensurate with the accumulation of CD8 T cells in the liver. Given that the DC accumulation in the liver was observed late in the response (>60 days post-immunisation), this effect is unlikely to contribute to the crucial γδ T cell-dependent priming observed in the current study.

Prior to the discovery of T_{RM} cells, a role for IL-4 in RAS vaccination (for *P. yoelii* in BALB/c mice[46,57]) was identified. CD4 T cells, rather than γδ T cells, were implicated as the source of IL-4[46,57]. We speculate that a lack of CD40L signalling in the absence of CD4 T cells, rather than a lack of CD4 T cell-derived IL-4, was likely responsible for the phenotype observed. However, we currently cannot exclude the possibility that γδ T cell-derived IL-4 drives production of IL-4 by CD4 T cells. Nevertheless, we have shown that the initial and most important source of IL-4 is γδ T cell-derived.

Notably, we have shown that IL-4 and IL-12 are synergistic for CD8 T cell expansion due to enhanced expression of IL-12R, likely making the T cells more sensitive to bioactive IL-12. This is counterintuitive to published literature examining CD4 T cell responses, which states that IL-4-induced GATA3 activation suppresses IL-12 signalling[58]. However, synergistic effects of IL-4 and IL-12 have previously been reported for CD4 T cells[59] and human T cells[60], although the precise molecular mechanisms driving this synergy are currently unknown and require further investigation. Here, we show that IL-4 plays a key role in promoting the expansion of antigen-specific T cells by not only stimulating IL-12 production in DC but also enhancing $CD8^+$ T cell sensitivity to the IL-12 produced. In the absence of IL-4 the entire response fails, making IL-4, and the triggers that induce its secretion by γδ T cells or other innate or innate-like cells, of major relevance to weakly stimulating pathogens (or tumours) that cannot intrinsically drive strong CD8 responses.

Importantly, a newly appreciated role for IL-4 in the context of immunotherapy has recently been highlighted. IL-4 production by B cells was shown to be one mechanism for successful

487 PD-1 immunotherapy[61] and two recent studies demonstrated the importance of an IL-4 driven
488 type-2 response for effective and long-lived CAR T or anti-tumour responses[62,63]. These studies
489 demonstrate that IL-4 has therapeutic implications beyond infectious diseases and indicate that
490 γδ T cells should be investigated as a source of IL-4 in these models.
491
492 In conclusion, our study reveals that by providing IL-4, Vγ1+ γδ T cells drive the initiation of
493 the response to a poorly immunogenic pathogen, transforming it into a robust trigger for $CD8^+$
494 T cell immunity and tissue-tropic memory.
495
496 **Methods**
497 **Mice, mosquitoes, and parasites**
498 C57BL/6, B6.SJL-PtprcaPep3b/BoyJ (CD45.1), PbT-I GFP, PbT-II GFP, *Tcrd*$^{-/-}$[64],
499 Trdc$^{tm1(EGFP/HBEGF/luc)Impr}$ (TCRδ-GDL)[65], *Il4*$^{-/-}$, *Batf3*$^{-/-}$, *Cd40l (Cd154)*$^{-/-}$, *Il17a*$^{-/-}$ mice were
500 bred and held at the Department of Microbiology and Immunology and the University of
501 Melbourne. All experimental work and animal handling was conducted in strict accordance
502 with the standards approved by the Animal Ethics Committee at the University of Melbourne
503 (ethic project ID: 2015168, 20088). Experimental mice were sex matched and used at 6-12 wks
504 of age. Both male and female mice were used. TCRδ-GDL[65] mice were kindly provided by I.
505 Prinz (University Medical Center Hamburg-Eppendorf). *Il4*$^{-/-}$ mice (JAX), were backcrossed to
506 B6 mice for >10 generations prior to acquisition for this study.
507
508 **Generation of Pb*Δmei2* parasites**
509 Pb*Δmei2* parasites were generated. The following was performed with the gene region for *mei2*
510 reversed so that the coding sequence reads left to right. 5' and 3' homology flanks were
511 amplified from Pb genomic DNA with the primers CJ472 + CJ473, and CJ474 + CJ475
512 (**Supplementary Table 1**), producing amplicons of 798bp and 832bp respectively. The 5' flank
513 reverse primer CJ473 and the 3' flank forward primer CJ474 both featured a 23 base multi-
514 cloning-site complementary tail (including a possible guide sequence), which was utilized in a
515 further PCR reaction to generate the 5', 3' flank fusion fragment. This was cloned into the
516 CRISPR/Cas9 plasmid pYC_L2 (a kind gift from Ashley Vaughan) with the restriction
517 enzymes *Kpn*I and *Eco*RI. Two guide sequences (Guide 3 and 28) were identified with
518 CHOPCHOP[66] and each sequence cloned into separate KO flank containing plasmids with the
519 enzyme Esp3I to generate the mei2KO plasmid pCJ133 and 134 respectively. 15ug of each

520 plasmid was co-tranfected into into magnet-purified Pb schizont stage parasites as previously
521 described[67,68] and injected intravenously into Swiss Webster mice. After 24 hours, mice were
522 put on water containing 70 µg/mL pyrimethamine. When mice reached >1% parasitemia they
523 were euthanized and cryostocks prepared. Genotyping was performed by PCR (primers in
524 **Supplementary Table 1**) and clonal parasites generated by limiting dilution as previously
525 described[69].
526
527 For the generation of fresh sporozoites, 4-5 wk old Swiss Webster mice were purchased from
528 the Monash Animal Services (Melbourne, Victoria, Australia) and maintained at the School of
529 Biosciences, The University of Melbourne, Australia. *Anopheles stephensi* mosquitoes (strain
530 STE2/MRA-128 from The Malaria Research and Reference Reagent Resource Center) were
531 reared and infected with WT (*P. berghei* ANKA) or PbΔ*mei2* at the School of Biosciences, The
532 University of Melbourne. Sporozoites were dissected from mosquito salivary glands and
533 resuspended in PBS. For RAS experiments, freshly collected WT sporozoites were irradiated
534 with 20,000 rad using a gamma ^{60}Co source. For vaccination, mice were injected intravenously
535 with 2.5-5x10^4 RAS or 2 x10^4 PbΔ*mei2*.
536
537 **Cell Enrichments**
538 **T cells**
539 Naïve $CD8^+$ PbT-I or $CD4^+$ PbT-II cells were negatively enriched from the spleens and lymph
540 nodes of PbT-I-uGFP, OT-I/uGFP or PbT-II/uGFP transgenic mice. Briefly, cells were passed
541 through a 70 µM filter sieve to obtain a single-cell suspension and red blood cells (RBC) lysed.
542 Single-cell suspensions were labelled with rat monoclonal antibodies specific for MHC Class
543 II (M5-114), Mac-1 (M1/70, F4/80), Gr-1 (RB6-8C5) and either CD4 (GK1.4) (for PbT-I and
544 OT-I CD8 T cells) or CD8 (53-6.7) (for PbT-II CD4 T cells) prior to incubation with BioMag
545 goat anti-rat IgG coupled magnetic beads (Qiagen) and magnetic separation. Enriched T cells
546 were typically 80-90% pure. 1 x10^6 purified T cells in 200 µL of sterile PBS were injected via
547 the tail vein into recipient mice. Where co-transfers were performed, a total number of 2 x10^6
548 purified T cells were injected via the tail vein where cell types were transferred at a ratio of 1:1.
549
550 **γδ T cells**
551 Naïve γδ T cells were negatively enriched from spleens of B6 or *Il4*$^{-/-}$ mice. Single cell-
552 suspensions were achieved by finely mincing and digesting spleens in 1mg/mL Collagenase

553 Type 3, 20 μg/mL DNase I supplemented with a competitive antagonist of $P2X_7R$ (A-438079
554 hydrochloride; Santa Cruz Biotechnology) with intermittent agitation. Undigested fragments
555 were removed by filtering through a 70 μM mesh followed by red blood cell lysis. Single cell
556 suspensions were labelled with rat monoclonal antibodies specific for MHC Class II (M5-114),
557 Mac-1 (M1/70, F4/80), CD4 (GK1.4), CD8 (53-6.7) and B220 (RA3-6B2) prior to incubation
558 with BioMag goat anti-rat IgG coupled magnetic beads (Qiagen) and magnetic separation.
559 $2x10^6$ enriched γδ T cells in 200 μL of sterile PBS were injected via the tail vein into recipient
560 mice.
561
562 **Dendritic cells**
563 Dendritic cells were isolated from spleens of B16.Flt3L tumour-bearing mice. Briefly, spleens
564 were finely minced in 1mg/ml Collagenase Type 3, 20 μg/ml DNase I and continuously agitated
565 for 15 minutes. DC-T cell complexes were disrupted with the addition of 0.1M EDTA (pH7.2).
566 Undigested fragments were removed by filtering through a 70 μM mesh before light-density
567 separation with $1.077g/cm^3$ Nycodenz medium via centrifugation at 1700rpm at 4°C for 12min.
568 To increase the purity of cDC1 precursors, the light density fraction was collected, and
569 cDC1s/pre-cDC1s were negatively enriched for through incubation with rat mAb against CD3ε
570 (KT3), Thy1.1 (T24/31.7), Gr-1 (RB6-8C5), B220 (RA3-6B2), Ter-119 and CD11b (M1/70)
571 prior to incubation with BioMag goat anti-rat IgG coupled magnetic beads (Qiagen) and
572 magnetic separation. Target cells were characterised as $CD11c^+$, $MHC\text{-}II^{int/+}$, $CD11b^-$, $CD24^{hi}$,
573 $CD8\alpha^+$ with purities ranging between 60-80%. 2-5 x 10^6 purified cDC1s in 200 μL of sterile
574 PBS were injected via the tail vein into recipient mice, 2 days prior to PbT-I cell transfer.
575
576 **CRISPR/Cas9 gene-editing**
577 **T cells**
578 Purified $CD8^+$ PbT-I or $CD4^+$ PbT-II cells were gene-edited via electroporation with single
579 guide (sg) RNA ribonucleoproteins (RNPs) (sgRNA/Cas9 RNPs). Briefly, sgRNA/Cas9 RNPs
580 were formed in Nuclease-free H_2O using 0.6 μl of Alt-R S.*pyogenes* Cas9 Nuclease V3
581 (10mg/mL, Integrated DNA Technologies) incubated with 0.3 nmol of sgRNA targeting either
582 *Il4rα* (5'-AGUGGAGUCCUAGCAUCACG-3', 3'-AUCCAGGAACCACUCACACG-5') or
583 *Cd19* (5'-AAUGUCUCAGACCAUAUGGG-3') purchased from Synthego (CRISPRevolution
584 sgRNA EZ Kit) for 10 mins at room temperature. For each sgRNA/Cas9 electroporation
585 reaction, 10 x 10^6 target cells were required. In each reaction, target cells were resuspended in

586 20 µl of reconstituted P3 buffer then mixed with the sgRNA/Cas9 RNP complex and
587 electroporated using a Lonza 4D-Nucleofector (program code: DN100). Electroporated cells
588 were then rested in a 96-well plate for at least 10 minutes at 37°C. For injection into mice, 10^6
589 cells were injected into mice via the tail vein in 200 µL of PBS, one day prior to RAS
590 vaccination.
591
592 **Dendritic Cells**
593 Purified pre-cDC1s were gene-edited via electroporation with single guide (sg) RNA
594 ribonucleoproteins (RNPs) (sgRNA/Cas9 RNPs) using an optimised protocol. sgRNA/Cas9
595 RNPs were formed as described for T cell gene-editing. For each sgRNA/Cas9 electroporation
596 reaction, 10 x 10^6 target cells were required. In each reaction, target cells were resuspended in
597 20 µl of reconstituted P3 buffer then mixed with the sgRNA/Cas9 RNP complex and
598 electroporated using a Lonza 4D-Nucleofector (program code: CM137). Electroporated cells
599 were then rested in a 96-well plate for at least 20 minutes at 37°C then injected intravenously
600 into *Batf3*$^{-/-}$ mice three days prior to immunisation. All mice received PbT-Is and/or PbT-IIs one
601 day prior to RAS immunisation.
602
603 ***In vitro* cDC1 gene-expression assay**
604 Dendritic cells were isolated through the protocol outlined above. CD11c$^+$, MHC-II$^{int/+}$,
605 CD11b$^-$, CD24^{hi}, B220$^-$, CD172α$^-$ cells were then sorted using a BD FACSAria^{TM} III Cell
606 Sorter into filtered RPMI supplemented with 50% heat-inactivated FCS and pelleted. In a 24-
607 well plate, 5 x 10^5 cells were plated in complete Kenneth D Shortman RPMI (KDS-RPMI 1640,
608 10% FCS, 2 mM L-glutamine, 100 U/ml penicillin, 100 mg/mL streptomycin and 50 mM 2-
609 mercaptoethanol). To assess cDC1 gene expression in response to IL-4, cells were incubated in
610 the presence of α-CD40 (10 µg/ml), recombinant mouse IL-4 (60 ng/mL), IFN-γ (20 ng/mL),
611 or LPS (1 µg/ml). Plates were then incubated at 37°C and 5% CO_2 for 4 hours. For RNA
612 isolation, cells were washed and resuspended using TRIzol (Life Technologies), snap frozen
613 and stored at -80°C.
614
615 **RNA Isolation and sequencing**
616 To determine gene expression in cDC1s, mRNA was extracted using a Direct-zol RNA
617 MicroPrep kit (Zymo Research) as per manufacturer's protocol. Libraries were prepared using
618 Illumina stranded mRNA library kits and the outputs sequenced to a depth of 20M reads per

619 sample on a 150PE on Illumina NovaSeq X Plus 10B flow cell. Library preparation and
620 sequencing was conducted at the Australian Genome Research Facility.
621
622 **Bioinformatics Analyses**

623 Sequencing reads were aligned to the GRCm39 reference genome and transcriptome (version
624 105) using the STAR aligner (version 2.7.8a)[70] and transcript counts established using
625 featureCounts from the subread package (version 2.0.0)[71]. The data was then analysed using R
626 (version 4.2.0), limma (version 4.54.1)[72] and plots generated with ggplot2[73]. We first merged
627 technical replicates from separate sequencing lanes into their respective biological replicates
628 by summing up the counts. To obtain differentially expressed genes between the experimental
629 groups, the data were filtered for lowly or non-expressed genes (filterByExpr function) and
630 normalised counts by Trimmed Mean of M-values (TMM). Mean-variance trends were
631 estimated with the voom function and a linear model was fit using lmFit. The model parameters
632 were moderated using eBayes, p values corrected for multiple testing using the Benjamini-
633 Hochberg method and differential genes obtained for each of the pairwise contrasts between
634 the experimental groups. The heatmap of expression values of top differential genes was
635 generated with the pheatmap package (version 1.0.12) on log2 normalised CPM values.
636
637 **Bone-marrow chimeras**

638 Mice were irradiated with two doses of 550 rad 3 hours apart. Mice were reconstituted with 3-
639 5 x 10^6 bone marrow (BM) cells from either B6.Ly5.1, *Il4*$^{-/-}$ or *Tcrd*$^{-/-}$ mice. In the case of mixed
640 bone-marrow chimeras, mice were reconstituted with a 1:1 ratio of bone-marrow cells from
641 B6.Ly5.1, *Il4*$^{-/-}$ and/or *Tcrd*$^{-/-}$ mice totalling to 3-5 x 10^6 BM cells per mouse. BM cells were
642 prepared by removing the tibia and femur of donor mice. Bones were flushed with complete
643 RPMI using a 23G needle and a 10 mL syringe to collect bone marrow. Large chunks were
644 removed by passing cells through a 70 µM mesh filter. T cells were removed by resuspending
645 the pellet with Abs against CD4 (RL172), CD8α (3.168), and Thy1.1 (Jlj) for 30 minutes at
646 4°C followed by incubation with rabbit complement for 20 minutes at 37°C to remove bound
647 cells. All irradiated mice were injected via the tail vein with 3-5 x 10^6 bone marrow cells in 200
648 µL of PBS. The following day, all mice were injected intraperitoneally with 100 µL of T24 (α-
649 Thy1.1). Irradiated mice received antibiotic water containing 2.5 g/L Neomycin Sulphate and
650 0.94 g/L Polymyxin B sulphate for the first 4 weeks after irradiation followed by normal water
651 for at least another 4 weeks prior to experimental work.

652

653 ***In vivo* antibody depletion/blockade**

654 Mice were treated intraperitoneally with purified α-IL-4 (clone 11B11) for 6 days starting one
655 day prior to RAS vaccination. For the first 3 days, mice were treated with 500 µg then 200 µg
656 for the final 3 days. Control mice were treated with α-horseradish peroxidase (clone HRPN)
657 using the same dose and regimen[46].

658 For IL-12p40 neutralisation, mice were treated intraperitoneally with 250 µg of purified α-IL-
659 12p40 (clone C17.8) for 2 days beginning one day prior to RAS vaccination with an additional
660 dose the day prior to the end point. Control mice were treated with of α-trinitrophenol (clone
661 2A3) at the same dose and schedule[74].

662 To block γδ T cell function *in vivo*, mice received a single 200 µg dose of α-GL3 (clone GL3)
663 or α-Vγ1 (clone 2.11)[75] intravenously on the day prior to immunisation with RAS. As a control,
664 separate mice were treated with 200 µg of Purified Armenian Hamster IgG (clone HTK888)[19].

665

666 **Organ processing and flow cytometry**

667 Single cell suspensions were prepared from spleen or livers by passing through 70 µM mesh
668 filters. For experiments in which splenic DCs were enumerated, spleens were finely minced in
669 1mg/ml Collagenase Type 3, 20 µg/ml DNase I and continuously agitated for 15 minutes. DC-
670 T cell complexes were disrupted with the addition of 0.1M EDTA (pH7.2) prior to filtration
671 through a 70 µM mesh. Liver preparation required an additional step to resuspend cells in 35%
672 isotonic Percoll and centrifugation at 500 rpm for 20 minutes at room temperature. Red blood
673 cells were removed from spleen and liver pellets and labelled with near-IR fixable dye to
674 exclude dead cells. Fluorochrome-conjugated monoclonal antibodies specific for TCRδ, CD3ε,
675 NK1.1, CD8α, CD4, B220, IL-4R, TCRβ, CD69, CD62L, CD44, CD27, Vγ1, Vγ4, CD11a,
676 CXCR6, CD11c, CD11b, XCR1, CD24, CD172a and MHC-II were used for surface staining
677 and performed for an hour at 4°C. H2-K^b-$PbRPL6_{120-127}$, H2-D^b-$PbTRAP_{130-138}$, H2-D^b-
678 $PbGAP50_{40-48}$ tetramers were made by Stephanie Gras. Sphero Blank Calibration beads were
679 used to generate cell counts. Cells were acquired on a Cytek Aurora using the SpectroFlo v3.0
680 system (Cytek) and further analysed on FlowJo (TreeStar, Inc).

681

682 **In-vitro activation and culture of T cells**

683

684 PbT-I T cells were activated in complete RPMI (RPMI 1640, 10% FCS, 2mM L-glutamine,
685 100 U/ml penicillin, 100 mg/ml streptomycin and 50 mM 2-mercaptoethanol) for up to 6 days
686 with PbRPL6$_{120-127}$ (NVFDFNNL) peptide-pulsed splenocytes and in the presence of LPS (1
687 μg/ml; Sigma-Aldrich) and either: no added cytokine, recombinant mouse IL-12 (10 ng/mL[76]),
688 recombinant mouse IL-4 (60 ng/mL[42]; BioLegend) or both IL-12 and IL-4. Activated cells were
689 fed with complete RPMI on day 3 and split on day 4. To assess phenotype, cells were washed
690 and labelled with near-IR fixable dye to exclude dead cells and fluorochrome-conjugated
691 monoclonal antibodies specific for TCRβ, IL-4R, IL-12R, CD44, Vα8.3, and CD8α.
692
693 **Statistical Analyses**
694 Statistical analyses of graphed data were performed using GraphPad Prism software. Data are
695 shown as mean values ± SD. The statistical tests used, and p values are indicated in each figure
696 legend. All statistical tests were performed on log-transformed data unless otherwise specified.
697
698 **Acknowledgments**
699 The work was supported by The Australian National Health and Medical Research Council
700 (Grant #1105817 and 2002682) and The Australian Research Council (Grant #DP220103545).
701 S.G. is supported by an NHMRC SRF fellowship (#1159272). We wish to acknowledge the
702 University of Melbourne Bioresources platform and the Melbourne Cytometry platform for
703 support and expertise. We also wish to thank Melanie Damtsis and Gayle Davey for all the
704 indirect contributions that make great research possible and Dr Yannick Alexandre for critical
705 reading of the manuscript.
706
707 **Author Contributions**
708 SL performed the experiments with help from DM, SLiu, ZG, RM and LB and wrote the draft
709 of the paper. AC provided RAS and CJ made the genetically attenuated parasites both under
710 supervision by GM. CX and TB contributed methodology supervised by FK or LM. SG and IP
711 provided resources. JS conducted bioinformatic analysis of the RNAseq data. AB, SB, IC and
712 DFR helped with conceptualization and methodology. WRH and LB conceptualized, funded
713 and supervised the study and wrote the paper.
714
715 **Declaration of Interests**
716 The authors declare no competing interests.

717 **Figure Legends**

718

719 **Figure 1 - γδ T cells are essential for liver T_{RM} cell generation.**

720 (**A and C**) Numbers of (**A**) RPL6 (**C**) TRAP tetramer positive $CD8^+$ T cells in the liver of B6
721 or *Tcrd*$^{-/-}$ mice, 23 days after immunisation with 5 x10^4 RAS.

722

723 (**B and D**) Numbers of memory T cell (T_{MEM}) subsets; central memory T_{CM} ($CD62L^+$, $CD69^-$),
724 effector memory T_{EM} ($CD62L^-$, $CD69^-$) and resident memory T_{RM} ($CD62L^-$, $CD69^+$) within the
725 (**B**) RPL6 or (**D**) TRAP tetramer positive $CD44^+$ $CD8^+$ T cell compartment in the liver of B6 or
726 *Tcrd*$^{-/-}$ mice.

727

728 (**E**) Experimental Design for (**F**). B6 or *Tcrd*$^{-/-}$ mice were immunised with 2 x 2.5 x10^4 RAS
729 doses 2 weeks apart before challenge with 1 x10^3 live sporozoites on day 49. A parallel group
730 of unvaccinated (Nv) mice were also challenged.

731

732 (**F**) Parasitaemia in naïve (Nv) or RAS-vaccinated B6 or *Tcrd*$^{-/-}$ mice, 7 days after challenge
733 with 1 x10^3 P.*berghei* sporozoites.

734

735 (**G**) Numbers of RPL6 tetramer positive $CD8^+$ T cells in the liver of B6 or *Tcrd*$^{-/-}$ mice, 35 days
736 after vaccination with 2x10^4 P.*b*Δ*mei2*.

737

738 (**H**) Numbers of T_{CM}, T_{EM} and T_{RM} within the RPL6 positive $CD44^+$ $CD8^+$ T cell compartment
739 in the liver of B6 or *Tcrd*$^{-/-}$ mice, 35 days after vaccination with 2x10^4 P.*b*Δ*mei2*.

740

741 (**I and J**) 5x10^4 RPL6-specific transgenic $CD8^+$ T cells (PbT-I) were transferred into mice one
742 day prior to vaccination with 3.5 x10^4 RAS. Mice were culled 23 days after immunisation.
743 (**I**) Absolute numbers and (**J**) numbers of T_{CM}, T_{EM} and T_{RM} within PbT-I cells in the liver of
744 B6 or *Tcrd*$^{-/-}$ mice.

745

746

747 Data are pooled from (**A-D**) 3 independent experiments or (**F-J**) 2 independent experiments
748 with n = 6-14 mice per group. Error bars indicate mean + SEM. p values were calculated on

749 log-transformed data using an unpaired t test (A-D, G-J) or an ordinary one-way ANOVA (F).
750 ****$p<0.0001$, ***$p<0.001$, **$p<0.01$, *$p<0.05$, ns=$p>0.05$.
751
752 **Figure 2 - Splenic γδ T cells are activated within 24 hours of RAS vaccination.**
753 (**A and B**) 10^6 RPL6-specific transgenic $CD8^+$ T cells (PbT-I) were transferred into mice one
754 day prior to vaccination with 5 x10^4 RAS. Mice were culled and analysed 6 days later.
755 Absolute numbers of PbT-I cells in the (**A**) spleen or (**B**) liver of B6 or *Tcrd*$^{-/-}$ mice six days
756 after vaccination.
757
758 (**C**) Experimental design for (**D and E**). 10^6 transgenic $CD8^+$ T cells (PbT-I) and $CD4^+$ T cells
759 (PbT-II) were adoptively transferred into mice one day prior to vaccination with 5x10^4 RAS.
760 Mice were culled for analysis 6 days later.
761
762 (**D and E**) Numbers of (**D**) PbT-I or (**E**) PbT-II cells recovered from the spleen on day 6.
763
764 (**F**) Experimental design for (**G**). Mice received 10^6 PbT-I cells one day prior to vaccination
765 with RAS. Mice were given α-GL3 or an isotype control Ab either (i) before RAS, or (ii) 24
766 hours after RAS.
767
768 (**G**) Numbers of PbT-I cells in the spleen on day 6 post-vaccination.
769
770 (**H**) Representative FACS plots of $V\gamma1^+$ $CD11a^{hi}$ γδ T cells in naïve or RAS-vaccinated TCRδ-
771 GDL mice 24 hours after injection.
772
773 (**G**) Frequency of activated ($CD69^+$ $CD11a^{hi}$ $CD25^+$) $V\gamma1^+$ or $V\gamma1^-$ γδ T cells in naïve or RAS
774 vaccinated TCRδ-GDL mice 24 hours post-injection.
775
776 (**J**) Experimental design for (**K**)
777
778 (**K**) Normalised PbT-I cell numbers in the spleens 6 days post-vaccination in wild-type
779 "CTRL", a-Vg1-treated (clone 2.11) or α-pan-γδ-TCR treated (clone GL3) mice. Numbers
780 were normalised by expressing them as a fraction of the mean of the "CTRL" group.
781

Data is pooled from (**A, B**) 2 independent experiments, (**D-G**) 3 independent experiments, or (**I, K**) 4 independent experiments with n= 9-20mice per group. Error bars indicate mean + SEM. p values were calculated on log-transformed data using an unpaired t test (**A-E**), an ordinary one-way (**G, K**) or two-way (**I**) ANOVA. ****p<0.0001, ***p<0.001, **p<0.01, *p<0.05, ns=p>0.05.

Figure 3 - Antigen presentation and CD40-CD40L signalling is intact in the absence of γδ T cells.

10^6 CTV-labelled OVA-specific $CD8^+$ T (OT-I) cells were transferred into B6 or *Tcrd*$^{-/-}$ mice one day prior to vaccination with 50,000 CS5M-RAS. Mice were culled on day 1, day 2, day 3 and day 6 after transfer.

(**A**) Representative FACS plots of the $CD44^+$ OT-I cell compartment in the spleen at the indicated time points.

(**B, C**) (**B**) Frequency and (**C**) number of $CD69^+$ CTV^{hi} OT-I cells in the spleen of either B6 or *Tcrd*$^{-/-}$ mice across the indicated time points.

(**D**) Numbers of proliferated (CTV^{low}) OT-I cells in the spleen of either B6 or *Tcrd*$^{-/-}$ mice across the indicated time points.

(**E**) Experimental design for (**F**). B6, *Tcrd*$^{-/-}$ and *Cd40l* (*Cd154*)$^{-/-}$ mice received PbT-I cells with or without PbT-II cells co-transferred one day prior to vaccination with $5x10^4$ RAS.

(**F**) Numbers of PbT-I cells in the spleen at day 6 post-vaccination.

(**G**) CD40 signalling to DC is intact when CD40L sufficient T cells are provided, showing that CD4 T cells, not γδ T cells provide CD40L in this system.

Data is pooled from 2 independent experiments with (**A-D**) n = 8 or (**F**) n= 6 mice. Error bars indicate mean + SD. p values were calculated on log-transformed data using an unpaired t test (**D**) or an ordinary one-way ANOVA (**F**). ****p<0.0001, ***p<0.001, **p<0.01, *p<0.05, ns=p>0.05.

815 **Figure 4 - IL-4 is required for the CD8 T cell response to RAS vaccination.**
816 (**A**) Experimental design for (**B-D**). (**B**) 10^6 RPL6-specific $CD8^+$ T (PbT-I) cells were
817 transferred into B6, *Il4*$^{-/-}$ or *Tcrd*$^{-/-}$ mice one day prior to vaccination with $5x10^4$ RAS. An
818 additional cohort of *Il4*$^{-/-}$ received both 10^6 PbT-I cells and 10^6 PbT-II cells.
819
820 (**B**) Number of PbT-I cells in the spleen of B6, *Il4*$^{-/-}$ or *Tcrd*$^{-/-}$ mice at 6 days post-vaccination.
821
822 (**C and D**) Numbers of (**C**) PbT-I cells and (**D**) PbT-II cells in the spleen of B6, *Il4*$^{-/-}$ or *Tcrd*$^{-/-}$
823 mice that received both PbT-I and PbT-II cells.
824
825 (**E**) Experimental design for (**F and G**). Mice were irradiated twice with 550 rad and
826 reconstituted with $5x10^6$ bone-marrow (BM) cells. After an 8-week resting period, chimeric or
827 untreated mice were given 10^6 PbT-I cells one day prior to RAS vaccination, then culled 6 days
828 later. Chimeras were prepared with BM from either Ly5.1 (CD45.1) or *Tcrd*$^{-/-}$ donors.
829 (**F**) Numbers of γδ T cells in the spleens of wild-type mice (B6, *Tcrd*$^{-/-}$) and chimeras (Ly5.1→
830 B6, *Tcrd*$^{-/-}$ →Ly5.1) separated into $V\gamma1^-$ or $V\gamma1^+$ cells.
831
832 (**G**) Numbers of PbT-I cells in the spleens of non-chimeric (B6, *Tcrd*$^{-/-}$) or chimeric (Ly5.1→
833 B6, *Tcrd*$^{-/-}$ →Ly5.1) mice.
834
835 (**H**) Experimental design for (**I and J**). Mice were irradiated twice with 550 rad and
836 reconstituted with $5x10^6$ BM cells. After an 8-week resting period, chimeric mice were given
837 10^6 PbT-I cells one day prior to RAS vaccination then culled 6 days later. Chimeras were
838 prepared using bone marrow from B6, *Tcrd*$^{-/-}$, *Il4*$^{-/-}$ donors as indicated. Mixed B6 + *Tcrd*$^{-/-}$ and
839 *Il4*$^{-/-}$ + *Tcrd*$^{-/-}$ were prepared with a 50:50 mix of donor cells.
840
841 (**I**) Numbers of γδ T cells in the spleens of single and mixed chimeras separated into $V\gamma1^-$ or
842 $V\gamma1^+$ cells.
843 (**J**) Numbers of PbT-I cells in the spleens of chimeras 6 days after RAS vaccination.
844
845 (**K**) Experimental design for (**L and M**). *Tcrd*$^{-/-}$ mice received γδ T cells enriched from the
846 spleens of either B6 or *Il4*$^{-/-}$ donors one day prior to transfer of 10^6 PbT-I cells. The next day
847 mice were vaccinated with $5x10^4$ RAS and culled 6 days later.

848

849 (**L**) Absolute numbers of γδ T cells in the spleen 6 days after RAS vaccination in *Tcrd*$^{-/-}$ mice
850 that received γδ T cells from B6 (+γδ B6), or *Il4*$^{-/-}$ mice (+γδ *Il4*$^{-}$) or no γδ T cells (no transfer).
851

852 (**M**) Normalised PbT-I cell numbers in the spleen 6 days after RAS vaccination. Numbers were
853 normalised by expressing them as a fraction of the mean of the "+ γδ (B6)" group.
854

855 Data is pooled from **(B, I and J**) 4 independent experiments, **(C, D, L and M**) 3 independent
856 experiments, or (**F and G**) from 2 independent experiments where n=5-23 mice per group. Error
857 bars indicate mean + SEM. p values were calculated on log-transformed data using an ordinary
858 one-way ANOVA. ****p<0.0001, ***p<0.001, **p<0.01, *p<0.05, ns=p>0.05
859

860 **Figure 5 - CD8 T cells and dendritic cells respond directly to IL-4.**
861 (**A**) Experimental design for (**B-E**). 10^6 CD8$^+$ PbT-I and CD4$^+$ PbT-II CRISPR-Cas9 ablated
862 sg*Cd19* (control) or sg*Il4ra* cells were transferred into mice one day prior to vaccination with
863 5x10^4 RAS. All mice were culled on day 6 post-vaccination.
864

865 (**B**) Histogram of surface IL-4Ra expression on CRISPR-Cas9 ablated sg*Cd19* (control) or
866 sg*Il4ra* PbT-I cells, day 6 post-RAS.
867

868 (**C and D**) Numbers of (**C**) PbT-I and (**D**) PbT-II cells in the spleen on day 6 post-vaccination.
869

870 (**E**) Histogram of surface IL-4Ra expression on CRISPR-Cas9 ablated sg*Cd19* (control) or
871 sg*Il4ra* PbT-II cells, day 6 post-RAS vaccination.
872

873 (**F**) Experimental design for (**G and H**). *Batf3*$^{-/-}$ mice received 2x10^6 B16.Flt3L-elicted pre-
874 cDC1s (CD24$^+$ MHC-II$^+$ CD11c$^+$). Two days later, mice received 10^6 CD8$^+$ PbT-I cells and
875 5x10^4 RAS one day later. Mice were culled on day 6 post-RAS. For (**H**), cDC1s were
876 CRISPR-Cas9 edited using sg*Cd19* (control) or sg*Il4ra*.
877

878 (**G**) Number of PbT-I cells in the spleens of *Batf3*$^{-/-}$ mice that received pre-cDC1s (+ transfer)
879 or no pre-cDC1s (- transfer).
880

881 (**H**) Number of cDC1 recovered in the spleens of *Batf3*$^{-/-}$ mice that received CRISPR-Cas9
882 edited cDC1s (+sg*Cd19* or +sg*Il4ra*), or no pre-cDC1s (- transfer).
883
884 (**I**) Number of PbT-I cells in the spleens of *Batf3*$^{-/-}$ mice that received CRISPR-Cas9 edited
885 cDC1s, or no cDC1s (- transfer).
886
887 (**J**) IL-4 acts directly on CD8 T cells and cDC1s for CD8 T cell accumulation.
888
889 Data is pooled from (**B-E, H and I**) 2 independent experiments or (**G**) 4 independent
890 experiments where n=6-16 mice per group. Error bars indicate mean + SEM. p values were
891 calculated on log-transformed data using an ordinary one-way ANOVA. ****p<0.0001,
892 ***p<0.001, **p<0.01, *p<0.05, ns=p>0.05
893
894
895 **Figure 6 - CD40 and IL-4 drive a unique gene expression profile in cDC1**.
896 (**A**) Experimental design for (**B-D**).
897
898 (**B**) Heatmap showing expression of the 841 up-regulated and 762 down-regulated
899 differentially expressed genes (DEG) between media alone and CD40+IL-4, across the
900 different stimulation conditions.
901
902 (**C**) Volcano plot showing DEGs between αCD40 only and aCD40+IL-4 stimuli.
903
904 (**D**) Gene expression of *Il12a* across indicated stimuli combinations shown as counts per
905 million (CPM).
906
907 (**E**) Experimental design for (**F**). Mice received 10^6 PbT-I cells one day prior to RAS
908 vaccination and were administered αIL-12p40 on the day of T cell transfer, the day of RAS
909 vaccination then 5 days post-RAS.
910
911 (**F**) Number of PbT-I cells in the spleen on day 6 post-RAS vaccination.
912

913 (**G**) γδ T cell-derived IL-4 act on cDC1s to promote IL-12 production which, along with IL-4,
914 is required for $CD8^+$ T cell accumulation.
915
916 Data (**A-D**) is pooled from 3-5 independent experiments. (**A-D**) n= 3-5 sequencing replicates
917 derived from individual cDC1 cultures or (**F**) n=10 mice from 2 independent experiments. Error
918 bars indicate mean + SEM. p values were calculated on log-transformed data using an ordinary
919 one-way ANOVA. ****$p<0.0001$, ***$p<0.001$, **$p<0.01$, *$p<0.05$, ns=$p>0.05$.
920
921

922 **Figure 7 - IL-4 and IL-12 synergise to promote expansion of CD8 T cells.**
923 PbT-I T cells were activated *in vitro* in (**A**) media alone or in the presence of (**B**) 60ng/mL rmIL-
924 4, (**C**) 10ng/mL rmIL-12 or (**D**) both rmIL-4 and rmIL-12.
925
926 (**E**) IL-4R and (**F**) IL-12R surface expression on activated T cells 4 days after culture in the
927 presence of different cytokines.
928
929 OT-I T cells were activated *in vitro* in the presence of 60 ng/mL rmIL-4, 10 ng/mL rmIL-12 or
930 both rmIL-4 and rmIL-1 then transferred into mice at day 4 of culture. (**G**) Number of OT-I T
931 cells in the spleen 3 days after transfer.
932
933 (**H**) Experimental design for (**I-L**). Mice received 10^6 PbT-I cells one day prior to RAS
934 vaccination and were administered a-IL-12p40 or a-IL-4 according to the treatment regimen
935 depicted.
936
937 (**I and K**) Number of absolute PbT-I T cells in the (**I**) spleen and (**K**) liver, 29 days after
938 vaccination.
939
940 (**J and L**) Frequency of T_{CM}, T_{EM} and T_{RM} within the $CD44^+$ PbT-I T cell compartment in the
941 (**J**) spleen or (**L**) liver 29 days after RAS vaccination.
942
943 (**M**) γδ T cell-derived IL-4 act on cDC1s to promote IL-12 production which, along with IL-4,
944 signals directly on $CD8^+$ T cells to drive proliferation and therefore enhance liver T_{RM}
945 formation.
946
947 Data is pooled from (**A**) 5 independent experiments, (**E and F**) 4 independent experiments, (**G**)
948 3 independent experiments or (**I-K**) 2 independent experiments where (A-F) n = 4-5 individual
949 cultures per group or (G-L) n = 6-9 mice per group. Error bars indicate mean + SEM. p values
950 were calculated on log-transformed data using (**A-D**) a paired t test or (**E-L**) an ordinary one-
951 way ANOVA. ****$p<0.0001$, ***$p<0.001$, **$p<0.01$, *$p<0.05$, ns=$p>0.05$
952
953 **Figure S1 – Related to Figure 1; gd T cells are essential for liver T_{RM} cell generation.**
954 Mice were vaccinated with 1 dose of 5 x10^4 RAS. 35 days later, mice were culled.

955 (**A and B**) Representative FACS plots showing (**A**) RPL6 and (**B**) TRAP tetramer staining in
956 the liver in B6 or *Tcrd*$^{-/-}$ mice 35 days after RAS.
957
958 (**C and E**) Numbers of (**C**) RPL6 (**E**) TRAP tetramer positive CD8^{+} T cells in the spleen of B6
959 or *Tcrd*$^{-/-}$ mice, 35 days after RAS vaccination.
960 (**D and F**) Frequency of memory T cell (T_{MEM}) subsets; central memory T_{CM} (CD62L^{+}, CD69^{-}
961), effector memory T_{EM} (CD62L^{-}, CD69^{-}) and resident memory T_{RM} (CD62L^{-}, CD69^{+}) within
962 the (**D**) RPL6 and (**F**) TRAP tetramer positive CD44^{+} CD8^{+} T cell compartment in the spleen
963 of B6 or *Tcrd*$^{-/-}$ mice.
964
965 (**G**) Numbers of RPL6 tetramer positive CD8^{+} T cells in the spleen of B6 or *Tcrd*$^{-/-}$ mice, 35
966 days after vaccination with 2 x10^{4} P.*b*D*mei2*.
967
968 (**H**) Frequency of T_{CM}, T_{EM} and T_{RM} within the RPL6 tetramer positive CD44^{+} CD8^{+} T cell
969 compartment in the spleen of B6 or *Tcrd*$^{-/-}$ mice, 35 days after vaccination with 2 x10^{4}
970 P*b*Dmei2.
971
972 (**M**) Numbers of PbT-I cells in the spleen of B6 or *Tcrd*$^{-/-}$ mice, 23 days after immunisation with
973 5 x10^{4} RAS.
974 (**J**) Frequency of T_{CM}, T_{EM} and T_{RM} within the PbT-I T cell compartment in the spleen of B6 or
975 *Tcrd*$^{-/-}$ mice, 23 days after vaccination with 5 x10^{4} RAS.
976
977 Data is pooled from (**C-F**) 3 independent experiments or, (**G-J**) 2 independent experiments
978 where n = 6-14 mice per group. Error bars indicate mean + SEM. p values were calculated on
979 log-transformed data using an unpaired t test. ****p<0.0001, ***p<0.001, **p<0.01, *p<0.05,
980 ns=p>0.05.
981
982 **Figure S2 – Related to Figure 2; Splenic gd T cells are activated and mediate their effect**
983 **within 24 hours of RAS vaccination.**
984 (**A**) Numbers of PbT-I cells in the spleen of B6 or *Tcrd*$^{-/-}$ mice, 6 days after injection of irradiated
985 *P. berghei* infected red blood cells.
986
987 TCRd-GDL mice were vaccinated with 10^{5} RAS then culled 24 hours later.

988 (**B**) Representative FACS plots of gating strategy used to generate cell numbers in Figure S2B
989 and frequencies in Figure 2I.
990
991 (**C**) Number of activated (CD11a^{hi}, CD69^{+}, CD25^{+}) Vg1^{+} or Vg1^{-} gd T cells.
992
993 Relating to Figure 2(**C-D**), mice received 10^6 PbT-I and II cells one day prior to 5 x10^4 RAS
994 and were culled at day 6 post-immunisation. Numbers of (**D**) PbT-I or (**E**) PbT-II cells recovered
995 in the liver of B6 or *Tcrd*$^{-/-}$ mice.
996
997 Data is pooled from (**A**) 2 independent experiments, (**C**) 4 independent experiments or (**D-E**)
998 3 independent experiments where n = 5-13 mice per group. Error bars indicate mean + SEM. p
999 values were calculated on log-transformed data using a two-way ANOVA (**C**) or an unpaired t
1000 test (**D-E**). ****p<0.0001, ***p<0.001, **p<0.01, *p<0.05, ns=p>0.05.
1001
1002
1003 **Figure S3 – Related to Figure 3; Antigen presentation and CD40-CD40L signalling is**
1004 **intact in the absence of gd T cells.**
1005 10^6 CTV-labelled OVA-specific CD8^{+} T (OT-I) cells were transferred into B6 or *Tcrd*$^{-/-}$ mice
1006 one day prior to vaccination with 5 x10^4 RAS. Mice were culled on day 1, day 2, day 3 and day
1007 6 after transfer.
1008
1009 (**A-C**) Representative FACS plots of the CD44^{+} OT-I T cell compartment in the (**A**) liver-
1010 draining lymph-nodes, (**B**) liver, (**C**) inguinal lymph-node at the indicated time points.
1011
1012 (**D-F**) Numbers of proliferated (CTV^{low}) OT-I T cells in the (**D**) liver-draining lymph-nodes,
1013 (**E**) liver, (**F**) inguinal lymph-node of either B6 or *Tcrd*$^{-/-}$ mice across the indicated time points.
1014
1015 (**G-I**) Frequency of CD69^{+} CTV^{hi} OT-I T cells in the (**G**) liver-draining lymph-nodes, (**H**) liver,
1016 (**I**) inguinal lymph-node of either B6 or *Tcrd*$^{-/-}$ mice across the indicated time points.
1017
1018 Data is pooled from 2 independent experiments with n = 3-7 mice. Error bars indicate mean +
1019 SEM. p values were calculated on log-transformed data using an unpaired t test. **p<0.01,
1020 *p<0.05
1021

1022 **Figure S4 – Related to Figure 4; IL-4 is required for the CD8 T cell response to RAS**
1023 **vaccination.**
1024 (**A**) Experimental design for (**B**). Wild-type mice received 10^6 PbT-I cells and were vaccinated
1025 one day later with 5 x10^4 RAS. To determine the effect of blocking IL-4, mice were immunised
1026 with a-IL-4 (or isotype control) across 6 days beginning one day prior to RAS immunisation.
1027 500 µg was administered per day for the first 3 days and then 200 µg for the final 3 days. Mice
1028 were culled 6 days after RAS vaccination.
1029
1030 (**B**) Numbers of PbT-I cells in the spleen of isotype control and a-IL-4 treated mice 6 days after
1031 RAS vaccination.
1032
1033 Data is pooled from 4 independent experiments where n=8-14 mice per group. Error bars
1034 indicate mean + SEM. p values were calculated on log-transformed data using an ordinary one-
1035 way ANOVA (**B**) or an unpaired t test (**C**). ****p<0.0001, ***p<0.001, **p<0.01, *p<0.05,
1036 ns=p>0.05.
1037
1038 **Figure S5 – Related to Figure 5; CD8$^+$ T cells and dendritic cells respond directly to IL-**
1039 **4.**
1040
1041 (A) Representative FACS plots showing cDC1 gating on live, MHC-II$^+$ CD11c$^+$ in the spleen
1042 of *Batf3*$^{-/-}$ mice that received CRISPR-Cas9 edited pre-cDC1s (+sg*Cd19*, +sg*Il4ra*), or no pre-
1043 cDC1s (- transfer)
1044
1045
1046

1047 **Supplementary Table 1 – Primers used for the generation of Pb*Δmei2* parasites**

Name	Gene	F/R	Sequence	Purpose
CJ472	mei2	F	TATAGGTACCGTATGGGAACATGCATATTATGTGG	Forward to amplify the 5' flank of mei2 ko primer KpnI
CJ473	mei2	R	CCAACCTAGGTATAGGCGCGCCTACAAAAGGAATATGGGGAATACACC	Reverse for 5' Flank with linker including PAM site
CJ474	mei2	F	AGGCGCGCCTATACCTAGGTTGGGGATGTTTATAAATAAAATAGTGTAAAATTCG	3' Flank fwd with PAM linker
CJ475	mei2	R	atatGAATTCCCTGTTTAGGTTTATTTTGTCATTTCAC	3' flank rev with *Eco*RI
CJ562	mei2	F	GGCATGATGCCGAATGCC	Outside 5' flank for genotyping
CJ563	mei2	R	CATGTGTACACACGATCATATGG	Inside excised region downstream of 5' flank. Absent in KO
CJ564	mei2	F	GATGACCCGAGTTGTGAAGG	Inside excised region upstream of 3' flank. Absent in KO
CJ565	mei2	R	GAATTTTGAATATATGATCATATCGCACG	Outside 3' flank for genotyping
CJ566	mei2	R	CTAGGTATAGGCGCGCC	Inside linker to detect KO
CJ567	mei2	F	GCGCCTATACCTAGGTTGG	Inside linker to detect KO
CJ595	mei2	F	GCCTATACCTAGGTTGGGG	Alternative fwd in linker region of **Pb*Δmei2*** for KO genotyping
Mei2 KO guide 28	mei2	F	tattCATGTGTACACACGATCATA	Guide for mei2
Mei2 KO guide 28	mei2	R	aaacTATGATCGTGTGTACACATG	Guide for mei2
Mei2 KO Guide 3	mei2	F	tattAATGATGACCCGAGTTGTGA	Guide for mei2
Mei2 KO Guide 3	mei2	R	aaacTCACAACTCGGGTCATCATT	Guide for mei2

1048

1049

1050 **References**

1051 1. Joffre, O., Nolte, M.A., Sporri, R., and Reis e Sousa, C. (2009). Inflammatory signals in
1052 dendritic cell activation and the induction of adaptive immunity. Immunol Rev *227*,
1053 234-247. 10.1111/j.1600-065X.2008.00718.x.
1054 2. Bennett, S.R., Carbone, F.R., Karamalis, F., Flavell, R.A., Miller, J.F., and Heath, W.R.
1055 (1998). Help for cytotoxic-T-cell responses is mediated by CD40 signalling. Nature *393*,
1056 478-480. 10.1038/30996.
1057 3. Ridge, J.P., Di Rosa, F., and Matzinger, P. (1998). A conditioned dendritic cell can be a
1058 temporal bridge between a CD4+ T-helper and a T-killer cell. Nature *393*, 474-478.
1059 10.1038/30989.
1060 4. Schoenberger, S.P., Toes, R.E., van der Voort, E.I., Offringa, R., and Melief, C.J. (1998).
1061 T-cell help for cytotoxic T lymphocytes is mediated by CD40-CD40L interactions. Nature
1062 *393*, 480-483. 10.1038/31002.
1063 5. Reis e Sousa, C., Hieny, S., Scharton-Kersten, T., Jankovic, D., Charest, H., Germain, R.N.,
1064 and Sher, A. (1997). In vivo microbial stimulation induces rapid CD40 ligand-
1065 independent production of interleukin 12 by dendritic cells and their redistribution to
1066 T cell areas. J Exp Med *186*, 1819-1829. 10.1084/jem.186.11.1819.
1067 6. Albert, M.L., Jegathesan, M., and Darnell, R.B. (2001). Dendritic cell maturation is
1068 required for the cross-tolerization of CD8+ T cells. Nat Immunol *2*, 1010-1017.
1069 10.1038/ni722.
1070 7. Johnson, S., Zhan, Y., Sutherland, R.M., Mount, A.M., Bedoui, S., Brady, J.L., Carrington,
1071 E.M., Brown, L.E., Belz, G.T., Heath, W.R., and Lew, A.M. (2009). Selected Toll-like
1072 receptor ligands and viruses promote helper-independent cytotoxic T cell priming by
1073 upregulating CD40L on dendritic cells. Immunity *30*, 218-227.
1074 10.1016/j.immuni.2008.11.015.
1075 8. Rolph, M.S., and Kaufmann, S.H. (2001). CD40 signaling converts a minimally
1076 immunogenic antigen into a potent vaccine against the intracellular pathogen Listeria
1077 monocytogenes. J Immunol *166*, 5115-5121. 10.4049/jimmunol.166.8.5115.
1078 9. Overstreet, M.G., Chen, Y.C., Cockburn, I.A., Tse, S.W., and Zavala, F. (2011). CD4+ T
1079 cells modulate expansion and survival but not functional properties of effector and
1080 memory CD8+ T cells induced by malaria sporozoites. PLoS One *6*, e15948.
1081 10.1371/journal.pone.0015948.
1082 10. Weiss, W.R., Sedegah, M., Berzofsky, J.A., and Hoffman, S.L. (1993). The role of CD4+ T
1083 cells in immunity to malaria sporozoites. J Immunol *151*, 2690-2698.
1084 11. Murray, S.A., Mohar, I., Miller, J.L., Brempelis, K.J., Vaughan, A.M., Kappe, S.H., and
1085 Crispe, I.N. (2015). CD40 is required for protective immunity against liver stage
1086 Plasmodium infection. J Immunol *194*, 2268-2279. 10.4049/jimmunol.1401724.
1087 12. Clyde, D.F., Most, H., McCarthy, V.C., and Vanderberg, J.P. (1973). Immunization of man
1088 against sporozite-induced falciparum malaria. Am J Med Sci *266*, 169-177.
1089 10.1097/00000441-197309000-00002.
1090 13. Nussenzweig, R.S., Vanderberg, J., Most, H., and Orton, C. (1967). Protective immunity
1091 produced by the injection of x-irradiated sporozoites of plasmodium berghei. Nature
1092 *216*, 160-162. 10.1038/216160a0.
1093 14. Epstein, J.E., Tewari, K., Lyke, K.E., Sim, B.K., Billingsley, P.F., Laurens, M.B., Gunasekera,
1094 A., Chakravarty, S., James, E.R., Sedegah, M., et al. (2011). Live attenuated malaria
1095 vaccine designed to protect through hepatic CD8(+) T cell immunity. Science *334*, 475-
1096 480. 10.1126/science.1211548.

1097 15. Lau, L.S., Fernandez-Ruiz, D., Mollard, V., Sturm, A., Neller, M.A., Cozijnsen, A., Gregory,
1098 J.L., Davey, G.M., Jones, C.M., Lin, Y.H., et al. (2014). CD8+ T cells from a novel T cell
1099 receptor transgenic mouse induce liver-stage immunity that can be boosted by blood-
1100 stage infection in rodent malaria. PLoS Pathog *10*, e1004135.
1101 10.1371/journal.ppat.1004135.
1102 16. Jung, S., Unutmaz, D., Wong, P., Sano, G., De los Santos, K., Sparwasser, T., Wu, S.,
1103 Vuthoori, S., Ko, K., Zavala, F., et al. (2002). In vivo depletion of CD11c+ dendritic cells
1104 abrogates priming of CD8+ T cells by exogenous cell-associated antigens. Immunity *17*,
1105 211-220. 10.1016/s1074-7613(02)00365-5.
1106 17. Montagna, G.N., Biswas, A., Hildner, K., Matuschewski, K., and Dunay, I.R. (2015). Batf3
1107 deficiency proves the pivotal role of CD8alpha(+) dendritic cells in protection induced
1108 by vaccination with attenuated Plasmodium sporozoites. Parasite Immunol *37*, 533-
1109 543. 10.1111/pim.12222.
1110 18. Fernandez-Ruiz, D., Ng, W.Y., Holz, L.E., Ma, J.Z., Zaid, A., Wong, Y.C., Lau, L.S., Mollard,
1111 V., Cozijnsen, A., Collins, N., et al. (2016). Liver-Resident Memory CD8(+) T Cells Form
1112 a Front-Line Defense against Malaria Liver-Stage Infection. Immunity *45*, 889-902.
1113 10.1016/j.immuni.2016.08.011.
1114 19. Zaidi, I., Diallo, H., Conteh, S., Robbins, Y., Kolasny, J., Orr-Gonzalez, S., Carter, D., Butler,
1115 B., Lambert, L., Brickley, E., et al. (2017). gammadelta T Cells Are Required for the
1116 Induction of Sterile Immunity during Irradiated Sporozoite Vaccinations. J Immunol
1117 *199*, 3781-3788. 10.4049/jimmunol.1700314.
1118 20. Hayday, A.C. (2019). gammadelta T Cell Update: Adaptate Orchestrators of Immune
1119 Surveillance. J Immunol *203*, 311-320. 10.4049/jimmunol.1800934.
1120 21. Ribot, J.C., Lopes, N., and Silva-Santos, B. (2021). gammadelta T cells in tissue
1121 physiology and surveillance. Nat Rev Immunol *21*, 221-232. 10.1038/s41577-020-
1122 00452-4.
1123 22. Legut, M., Cole, D.K., and Sewell, A.K. (2015). The promise of gammadelta T cells and
1124 the gammadelta T cell receptor for cancer immunotherapy. Cell Mol Immunol *12*, 656-
1125 668. 10.1038/cmi.2015.28.
1126 23. Vantourout, P., and Hayday, A. (2013). Six-of-the-best: unique contributions of
1127 gammadelta T cells to immunology. Nat Rev Immunol *13*, 88-100. 10.1038/nri3384.
1128 24. Hayday, A.C. (2009). Gammadelta T cells and the lymphoid stress-surveillance
1129 response. Immunity *31*, 184-196. 10.1016/j.immuni.2009.08.006.
1130 25. Rigau, M., Ostrouska, S., Fulford, T.S., Johnson, D.N., Woods, K., Ruan, Z., McWilliam,
1131 H.E.G., Hudson, C., Tutuka, C., Wheatley, A.K., et al. (2020). Butyrophilin 2A1 is
1132 essential for phosphoantigen reactivity by gammadelta T cells. Science *367*.
1133 10.1126/science.aay5516.
1134 26. Lockhart, E., Green, A.M., and Flynn, J.L. (2006). IL-17 production is dominated by
1135 gammadelta T cells rather than CD4 T cells during Mycobacterium tuberculosis
1136 infection. J Immunol *177*, 4662-4669. 10.4049/jimmunol.177.7.4662.
1137 27. Azuara, V., Grigoriadou, K., Lembezat, M.P., Nagler-Anderson, C., and Pereira, P. (2001).
1138 Strain-specific TCR repertoire selection of IL-4-producing Thy-1 dull gamma delta
1139 thymocytes. Eur J Immunol *31*, 205-214. 10.1002/1521-4141(200101)31:1<205::AID-
1140 IMMU205>3.0.CO;2-8.
1141 28. Gerber, D.J., Azuara, V., Levraud, J.P., Huang, S.Y., Lembezat, M.P., and Pereira, P. (1999).
1142 IL-4-producing gamma delta T cells that express a very restricted TCR repertoire are
1143 preferentially localized in liver and spleen. J Immunol *163*, 3076-3082.

29. Heilig, J.S., and Tonegawa, S. (1986). Diversity of murine gamma genes and expression in fetal and adult T lymphocytes. Nature *322*, 836-840. 10.1038/322836a0.
30. Kalyan, S., and Kabelitz, D. (2013). Defining the nature of human gammadelta T cells: a biographical sketch of the highly empathetic. Cell Mol Immunol *10*, 21-29. 10.1038/cmi.2012.44.
31. Constant, P., Davodeau, F., Peyrat, M.A., Poquet, Y., Puzo, G., Bonneville, M., and Fournie, J.J. (1994). Stimulation of human gamma delta T cells by nonpeptidic mycobacterial ligands. Science *264*, 267-270. 10.1126/science.8146660.
32. Ishizuka, A.S., Lyke, K.E., DeZure, A., Berry, A.A., Richie, T.L., Mendoza, F.H., Enama, M.E., Gordon, I.J., Chang, L.J., Sarwar, U.N., et al. (2016). Protection against malaria at 1 year and immune correlates following PfSPZ vaccination. Nat Med *22*, 614-623. 10.1038/nm.4110.
33. Lyke, K.E., Ishizuka, A.S., Berry, A.A., Chakravarty, S., DeZure, A., Enama, M.E., James, E.R., Billingsley, P.F., Gunasekera, A., Manoj, A., et al. (2017). Attenuated PfSPZ Vaccine induces strain-transcending T cells and durable protection against heterologous controlled human malaria infection. Proc Natl Acad Sci U S A *114*, 2711-2716. 10.1073/pnas.1615324114.
34. Seder, R.A., Chang, L.J., Enama, M.E., Zephir, K.L., Sarwar, U.N., Gordon, I.J., Holman, L.A., James, E.R., Billingsley, P.F., Gunasekera, A., et al. (2013). Protection against malaria by intravenous immunization with a nonreplicating sporozoite vaccine. Science *341*, 1359-1365. 10.1126/science.1241800.
35. Sissoko, M.S., Healy, S.A., Katile, A., Omaswa, F., Zaidi, I., Gabriel, E.E., Kamate, B., Samake, Y., Guindo, M.A., Dolo, A., et al. (2017). Safety and efficacy of PfSPZ Vaccine against Plasmodium falciparum via direct venous inoculation in healthy malaria-exposed adults in Mali: a randomised, double-blind phase 1 trial. Lancet Infect Dis *17*, 498-509. 10.1016/S1473-3099(17)30104-4.
36. Valencia-Hernandez, A.M., Ng, W.Y., Ghazanfari, N., Ghilas, S., de Menezes, M.N., Holz, L.E., Huang, C., English, K., Naung, M., Tan, P.S., et al. (2020). A Natural Peptide Antigen within the Plasmodium Ribosomal Protein RPL6 Confers Liver TRM Cell-Mediated Immunity against Malaria in Mice. Cell Host Microbe. 10.1016/j.chom.2020.04.010.
37. Hafalla, J.C., Bauza, K., Friesen, J., Gonzalez-Aseguinolaza, G., Hill, A.V., and Matuschewski, K. (2013). Identification of targets of CD8(+) T cell responses to malaria liver stages by genome-wide epitope profiling. PLoS Pathog *9*, e1003303. 10.1371/journal.ppat.1003303.
38. Butler, N.S., Schmidt, N.W., Vaughan, A.M., Aly, A.S., Kappe, S.H.I., and Harty, J.T. (2011). Superior Antimalarial Immunity after Vaccination with Late Liver Stage-Arresting Genetically Attenuated Parasites. Cell Host & Microbe *9*, 451-462. 10.1016/j.chom.2011.05.008.
39. Franke-Fayard, B., Marin-Mogollon, C., Geurten, F.J.A., Chevalley-Maurel, S., Ramesar, J., Kroeze, H., Baalbergen, E., Wessels, E., Baron, L., Soulard, V., et al. (2022). Creation and preclinical evaluation of genetically attenuated malaria parasites arresting growth late in the liver. Npj Vaccines *7*. ARTN 139
10.1038/s41541-022-00558-x.
40. Valencia-Hernandez, A.M., Ng, W.Y., Ghazanfari, N., Ghilas, S., de Menezes, M.N., Holz, L.E., Huang, C., English, K., Naung, M., Tan, P.S., et al. (2020). A Natural Peptide Antigen within the Plasmodium Ribosomal Protein RPL6 Confers Liver TRM Cell-Mediated

Immunity against Malaria in Mice. Cell Host Microbe *27*, 950-962 e957. 10.1016/j.chom.2020.04.010.

41. Fernandez-Ruiz, D., Lau, L.S., Ghazanfari, N., Jones, C.M., Ng, W.Y., Davey, G.M., Berthold, D., Holz, L., Kato, Y., Enders, M.H., et al. (2017). Development of a Novel CD4(+) TCR Transgenic Line That Reveals a Dominant Role for CD8(+) Dendritic Cells and CD40 Signaling in the Generation of Helper and CTL Responses to Blood-Stage Malaria. J Immunol *199*, 4165-4179. 10.4049/jimmunol.1700186.
42. Enders, M.H., Bayarsaikhan, G., Ghilas, S., Chua, Y.C., May, R., de Menezes, M.N., Ge, Z., Tan, P.S., Cozijnsen, A., Mollard, V., et al. (2021). Plasmodium berghei Hsp90 contains a natural immunogenic I-A(b)-restricted antigen common to rodent and human Plasmodium species. Curr Res Immunol *2*, 79-92. 10.1016/j.crimmu.2021.06.002.
43. Koenecke, C., Chennupati, V., Schmitz, S., Malissen, B., Forster, R., and Prinz, I. (2009). In vivo application of mAb directed against the gammadelta TCR does not deplete but generates "invisible" gammadelta T cells. Eur J Immunol *39*, 372-379. 10.1002/eji.200838741.
44. Zheng, L., Hu, Y., Wang, Y., Huang, X., Xu, Y., Shen, Y., and Cao, J. (2017). Recruitment of Neutrophils Mediated by Vgamma2 gammadelta T Cells Deteriorates Liver Fibrosis Induced by Schistosoma japonicum Infection in C57BL/6 Mice. Infect Immun *85*. 10.1128/IAI.01020-16.
45. Cockburn, I.A., Tse, S.W., and Zavala, F. (2014). CD8+ T cells eliminate liver-stage Plasmodium berghei parasites without detectable bystander effect. Infect Immun *82*, 1460-1464. 10.1128/IAI.01500-13.
46. Carvalho, L.H., Sano, G., Hafalla, J.C., Morrot, A., Curotto de Lafaille, M.A., and Zavala, F. (2002). IL-4-secreting CD4+ T cells are crucial to the development of CD8+ T-cell responses against malaria liver stages. Nat Med *8*, 166-170. 10.1038/nm0202-166.
47. Morrot , A., Hafalla , J.C.R., Cockburn , I.A., Carvalho , L.H., and Zavala , F. (2005). IL-4 receptor expression on CD8+ T cells is required for the development of protective memory responses against liver stages of malaria parasites. Journal of Experimental Medicine *202*, 551-560. 10.1084/jem.20042463.
48. Haas, J.D., Ravens, S., Duber, S., Sandrock, I., Oberdorfer, L., Kashani, E., Chennupati, V., Fohse, L., Naumann, R., Weiss, S., et al. (2012). Development of interleukin-17-producing gammadelta T cells is restricted to a functional embryonic wave. Immunity *37*, 48-59. 10.1016/j.immuni.2012.06.003.
49. Woodward Davis, A.S., Bergsbaken, T., Delaney, M.A., and Bevan, M.J. (2015). Dermal-resident versus recruited gammadelta T cell response to cutaneous vaccinia virus infection. J Immunol *194*, 2260-2267. 10.4049/jimmunol.1402438.
50. Mach, N., Gillessen, S., Wilson, S.B., Sheehan, C., Mihm, M., and Dranoff, G. (2000). Differences in dendritic cells stimulated in vivo by tumors engineered to secrete granulocyte-macrophage colony-stimulating factor or Flt3-ligand. Cancer Res *60*, 3239-3246.
51. Gressier, E., Schulte-Schrepping, J., Petrov, L., Brumhard, S., Stubbemann, P., Hiller, A., Obermayer, B., Spitzer, J., Kostevc, T., Whitney, P.G., et al. (2023). CD4(+) T cell calibration of antigen-presenting cells optimizes antiviral CD8(+) T cell immunity. Nat Immunol *24*, 979-990. 10.1038/s41590-023-01517-x.
52. Mordmuller, B., Surat, G., Lagler, H., Chakravarty, S., Ishizuka, A.S., Lalremruata, A., Gmeiner, M., Campo, J.J., Esen, M., Ruben, A.J., et al. (2017). Sterile protection against

1237 human malaria by chemoattenuated PfSPZ vaccine. Nature *542*, 445-449.
1238 10.1038/nature21060.
1239 53. Zheng, H., Tan, Z., Zhou, T., Zhu, F., Ding, Y., Liu, T., Wu, Y., and Xu, W. (2015). The TLR2
1240 is activated by sporozoites and suppresses intrahepatic rodent malaria parasite
1241 development. Sci Rep *5*, 18239. 10.1038/srep18239.
1242 54. Kinjo, Y., Wu, D., Kim, G., Xing, G.W., Poles, M.A., Ho, D.D., Tsuji, M., Kawahara, K.,
1243 Wong, C.H., and Kronenberg, M. (2005). Recognition of bacterial glycosphingolipids by
1244 natural killer T cells. Nature *434*, 520-525. 10.1038/nature03407.
1245 55. Chora, A.F., Marques, S., Goncalves, J.L., Lima, P., Gomes da Costa, D., Fernandez-Ruiz,
1246 D., Marreiros, M.I., Ruivo, P., Carvalho, T., Ribeiro, R.M., et al. (2023). Interplay
1247 between liver and blood stages of Plasmodium infection dictates malaria severity via
1248 gammadelta T cells and IL-17-promoted stress erythropoiesis. Immunity *56*, 592-605
1249 e598. 10.1016/j.immuni.2023.01.031.
1250 56. Ribot, J.C., Neres, R., Zuzarte-Luis, V., Gomes, A.Q., Mancio-Silva, L., Mensurado, S.,
1251 Pinto-Neves, D., Santos, M.M., Carvalho, T., Landry, J.J.M., et al. (2019). gammadelta-
1252 T cells promote IFN-gamma-dependent Plasmodium pathogenesis upon liver-stage
1253 infection. Proc Natl Acad Sci U S A *116*, 9979-9988. 10.1073/pnas.1814440116.
1254 57. Morrot, A., Hafalla, J.C., Cockburn, I.A., Carvalho, L.H., and Zavala, F. (2005). IL-4
1255 receptor expression on CD8+ T cells is required for the development of protective
1256 memory responses against liver stages of malaria parasites. J Exp Med *202*, 551-560.
1257 10.1084/jem.20042463.
1258 58. Ouyang, W., Ranganath, S.H., Weindel, K., Bhattacharya, D., Murphy, T.L., Sha, W.C.,
1259 and Murphy, K.M. (1998). Inhibition of Th1 development mediated by GATA-3 through
1260 an IL-4-independent mechanism. Immunity *9*, 745-755. 10.1016/s1074-
1261 7613(00)80671-8.
1262 59. Oriss, T.B., McCarthy, S.A., Campana, M.A., and Morel, P.A. (1999). Evidence of positive
1263 cross-regulation on Th1 by Th2 and antigen-presenting cells: effects on Th1 induced by
1264 IL-4 and IL-12. J Immunol *162*, 1999-2007.
1265 60. Kriegel, M.A., Tretter, T., Blank, N., Schiller, M., Gabler, C., Winkler, S., Kalden, J.R., and
1266 Lorenz, H.M. (2006). Interleukin-4 supports interleukin-12-induced proliferation and
1267 interferon-gamma secretion in human activated lymphoblasts and T helper type 1
1268 cells. Immunology *119*, 43-53. 10.1111/j.1365-2567.2006.02404.x.
1269 61. Ruggiu, M., Guerin, M.V., Corre, B., Bardou, M., Alonso, R., Russo, E., Garcia, Z.,
1270 Feldmann, L., Lemaitre, F., Dusseaux, M., et al. (2024). Anti-PD-1 therapy triggers Tfh
1271 cell-dependent IL-4 release to boost CD8 T cell responses in tumor-draining lymph
1272 nodes. J Exp Med *221*. 10.1084/jem.20232104.
1273 62. Bai, Z., Feng, B., McClory, S.E., de Oliveira, B.C., Diorio, C., Gregoire, C., Tao, B., Yang,
1274 L., Zhao, Z., Peng, L., et al. (2024). Single-cell CAR T atlas reveals type 2 function in 8-
1275 year leukaemia remission. Nature *634*, 702-711. 10.1038/s41586-024-07762-w.
1276 63. Feng, B., Bai, Z., Zhou, X., Zhao, Y., Xie, Y.Q., Huang, X., Liu, Y., Enbar, T., Li, R., Wang, Y.,
1277 et al. (2024). The type 2 cytokine Fc-IL-4 revitalizes exhausted CD8(+) T cells against
1278 cancer. Nature *634*, 712-720. 10.1038/s41586-024-07962-4.
1279 64. Itohara, S., Mombaerts, P., Lafaille, J., Iacomini, J., Nelson, A., Clarke, A.R., Hooper,
1280 M.L., Farr, A., and Tonegawa, S. (1993). T cell receptor delta gene mutant mice:
1281 independent generation of alpha beta T cells and programmed rearrangements of
1282 gamma delta TCR genes. Cell *72*, 337-348. 10.1016/0092-8674(93)90112-4.

1283 65. Sandrock, I., Reinhardt, A., Ravens, S., Binz, C., Wilharm, A., Martins, J., Oberdorfer, L.,
1284 Tan, L., Lienenklaus, S., Zhang, B., et al. (2018). Genetic models reveal origin,
1285 persistence and non-redundant functions of IL-17-producing gammadelta T cells. J Exp
1286 Med *215*, 3006-3018. 10.1084/jem.20181439.
1287 66. Labun, K., Montague, T.G., Krause, M., Torres Cleuren, Y.N., Tjeldnes, H., and Valen, E.
1288 (2019). CHOPCHOP v3: expanding the CRISPR web toolbox beyond genome editing.
1289 Nucleic Acids Res *47*, W171-W174. 10.1093/nar/gkz365.
1290 67. Janse, C.J., Ramesar, J., and Waters, A.P. (2006). High-efficiency transfection and drug
1291 selection of genetically transformed blood stages of the rodent malaria parasite
1292 Plasmodium berghei. Nat Protoc *1*, 346-356. 10.1038/nprot.2006.53.
1293 68. Ribaut, C., Berry, A., Chevalley, S., Reybier, K., Morlais, I., Parzy, D., Nepveu, F., Benoit-
1294 Vical, F., and Valentin, A. (2008). Concentration and purification by magnetic
1295 separation of the erythrocytic stages of all human Plasmodium species. Malar J *7*, 45.
1296 10.1186/1475-2875-7-45.
1297 69. Sturm, A., Mollard, V., Cozijnsen, A., Goodman, C.D., and McFadden, G.I. (2015).
1298 Mitochondrial ATP synthase is dispensable in blood-stage Plasmodium berghei rodent
1299 malaria but essential in the mosquito phase. Proc Natl Acad Sci U S A *112*, 10216-
1300 10223. 10.1073/pnas.1423959112.
1301 70. Dobin, A., Davis, C.A., Schlesinger, F., Drenkow, J., Zaleski, C., Jha, S., Batut, P., Chaisson,
1302 M., and Gingeras, T.R. (2013). STAR: ultrafast universal RNA-seq aligner. Bioinformatics
1303 *29*, 15-21. 10.1093/bioinformatics/bts635.
1304 71. Liao, Y., Smyth, G.K., and Shi, W. (2013). The Subread aligner: fast, accurate and
1305 scalable read mapping by seed-and-vote. Nucleic Acids Res *41*, e108.
1306 10.1093/nar/gkt214.
1307 72. Law, C.W., Chen, Y., Shi, W., and Smyth, G.K. (2014). voom: Precision weights unlock
1308 linear model analysis tools for RNA-seq read counts. Genome Biol *15*, R29. 10.1186/gb-
1309 2014-15-2-r29.
1310 73. Wickham, H. Ggplot2 : elegant graphics for data analysis, Second edition. Edition.
1311 74. Taradi, M. (1981). [The influence of local factors on the growth of tumors (author's
1312 transl)]. Lijec Vjesn *103*, 212-213.
1313 75. Hao, J., Dong, S., Xia, S., He, W., Jia, H., Zhang, S., Wei, J., O'Brien, R.L., Born, W.K., Wu,
1314 Z., et al. (2011). Regulatory role of Vgamma1 gammadelta T cells in tumor immunity
1315 through IL-4 production. J Immunol *187*, 4979-4986. 10.4049/jimmunol.1101389.
1316 76. Diaz-Montero, C.M., El Naggar, S., Al Khami, A., El Naggar, R., Montero, A.J., Cole, D.J.,
1317 and Salem, M.L. (2008). Priming of naive CD8+ T cells in the presence of IL-12
1318 selectively enhances the survival of CD8+CD62Lhi cells and results in superior anti-
1319 tumor activity in a tolerogenic murine model. Cancer Immunol Immunother *57*, 563-
1320 572. 10.1007/s00262-007-0394-0.
1321

Figure 1

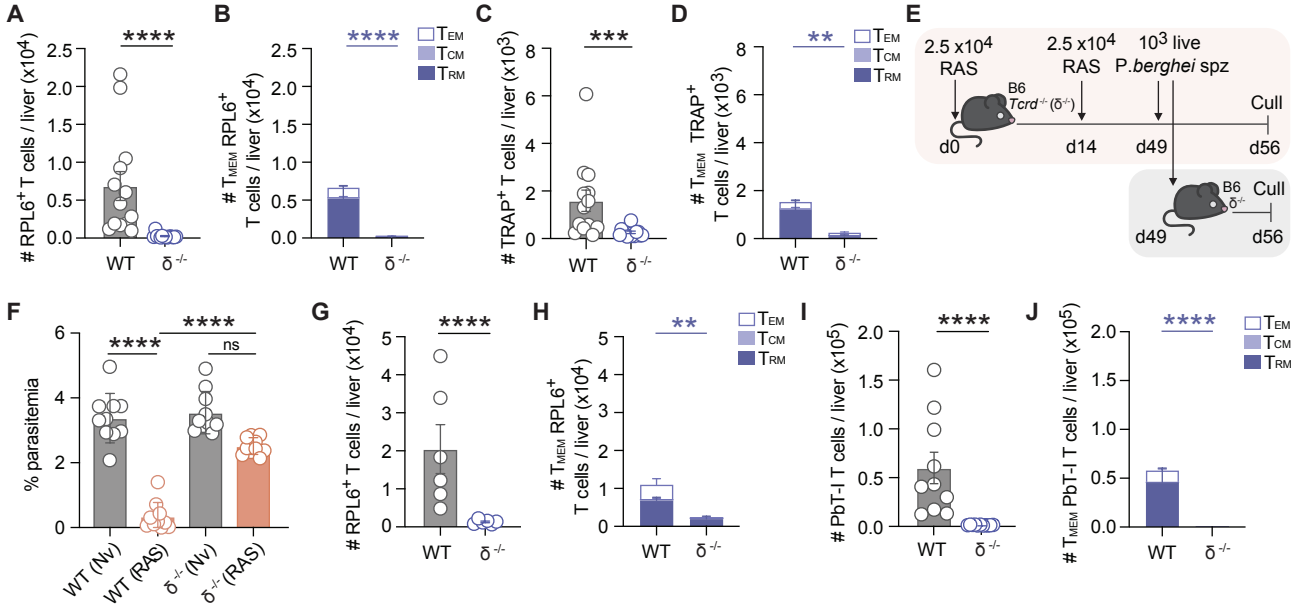
A
RPL6+ T cells / liver (x10^4)
****
WT
δ -/-
B
TMEM RPL6+ T cells / liver (x10^4)
****
TEM
TCM
TRM
C
TRAP+ T cells / liver (x10^3)
***
D
TMEM TRAP+ T cells / liver (x10^3)
**
E
2.5 x10^4 RAS
2.5 x10^4 RAS
10^3 live P.berghei spz
B6 Tcrd-/- (δ-/-)
Cull
d0
d14
d49
d56
B6 δ-/-
F
% parasitemia
****
ns
WT (Nv)
WT (RAS)
δ -/- (Nv)
δ -/- (RAS)
G
RPL6+ T cells / liver (x10^4)
H
TMEM RPL6+ T cells / liver (x10^4)
I
PbT-I T cells / liver (x10^5)
J
TMEM PbT-I T cells / liver (x10^5)

Figure 2

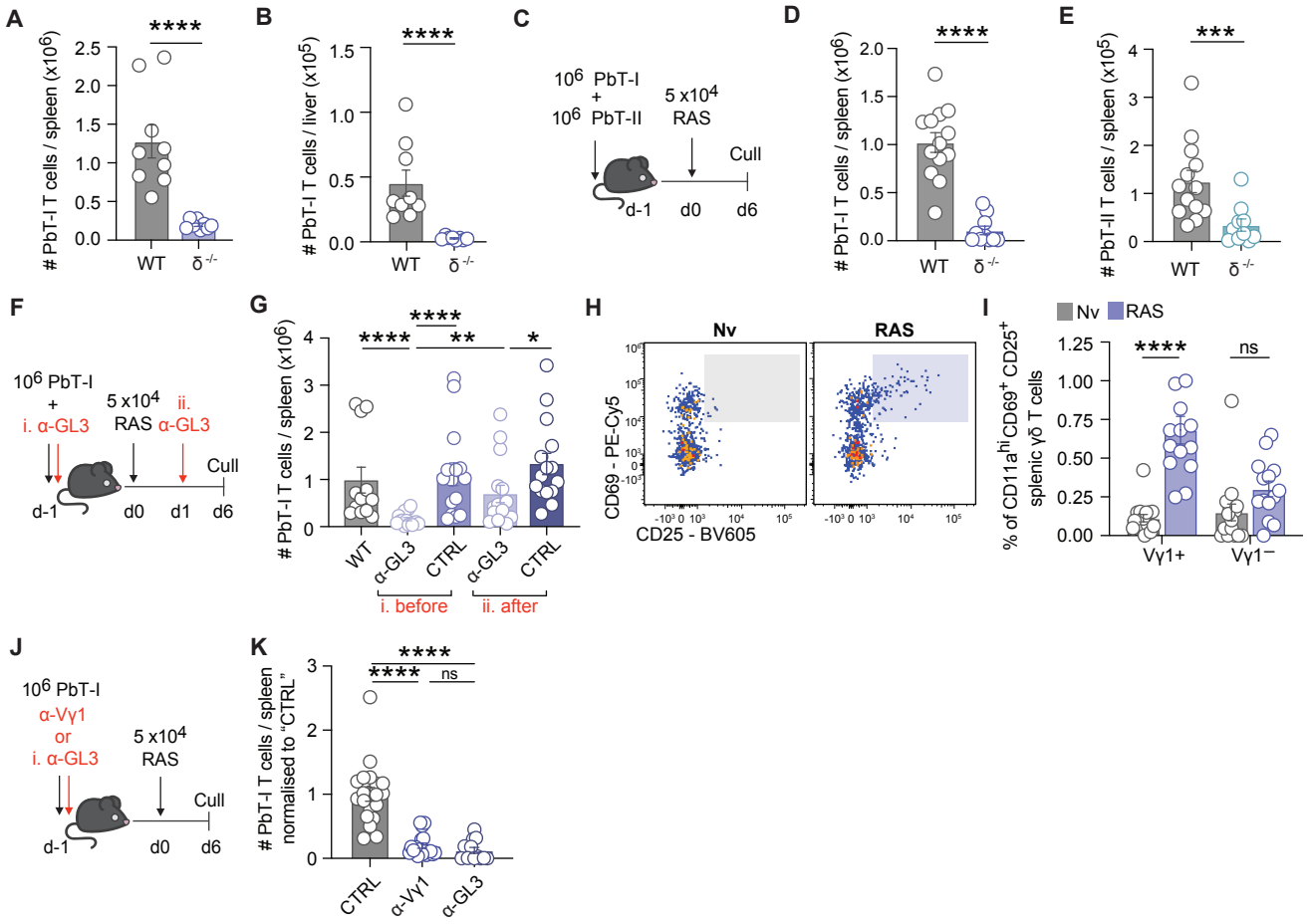
A
PbT-I T cells / spleen (x10^6)
****
WT
δ -/-
B
PbT-I T cells / liver (x10^5)
****
WT
δ -/-
C
10^6 PbT-I
+
10^6 PbT-II
5 x10^4
RAS
Cull
d-1
d0
d6
D
PbT-I T cells / spleen (x10^6)
****
WT
δ -/-
E
PbT-II T cells / spleen (x10^5)
***
WT
δ -/-
F
10^6 PbT-I
+
i. α-GL3
5 x10^4
RAS
ii.
α-GL3
Cull
d-1
d0
d1
d6
G
PbT-I T cells / spleen (x10^6)
****
****
**
*
WT
α-GL3
CTRL
α-GL3
CTRL
i. before
ii. after
H
Nv
RAS
CD69 - PE-Cy5
CD25 - BV605
I
Nv
RAS
% of CD11a^hi CD69^+ CD25^+ splenic γδ T cells
****
ns
Vγ1+
Vγ1−
J
10^6 PbT-I
α-Vγ1
or
i. α-GL3
5 x10^4
RAS
Cull
d-1
d0
d6
K
PbT-I T cells / spleen normalised to "CTRL"
****
****
ns
CTRL
α-Vγ1
α-GL3

Figure 3

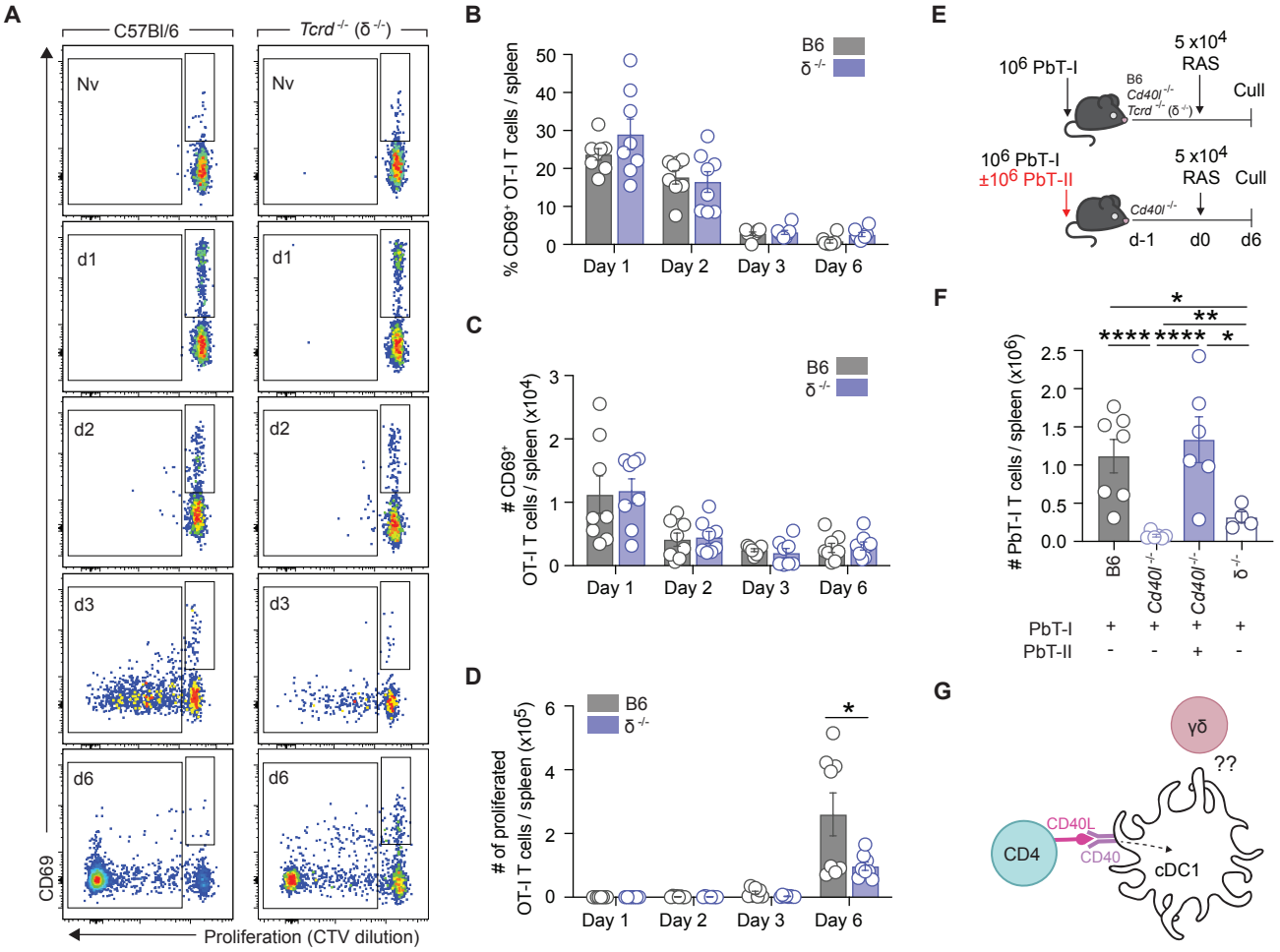
A
C57Bl/6
Tcrd -/- (δ -/-)
Nv
d1
d2
d3
d6
CD69
Proliferation (CTV dilution)
B
% CD69+ OT-I T cells / spleen
B6
δ -/-
Day 1
Day 2
Day 3
Day 6
C
CD69+ OT-I T cells / spleen (x10^4)
D
# of proliferated OT-I T cells / spleen (x10^5)
E
10^6 PbT-I
5 x10^4 RAS
Cull
B6
Cd40l -/-
Tcrd -/- (δ -/-)
10^6 PbT-I
±10^6 PbT-II
Cd40l -/-
d-1
d0
d6
F
PbT-I T cells / spleen (x10^6)
B6
Cd40l -/-
δ -/-
PbT-I
PbT-II
G
γδ
??
CD40L
CD40
CD4
cDC1

Figure 4

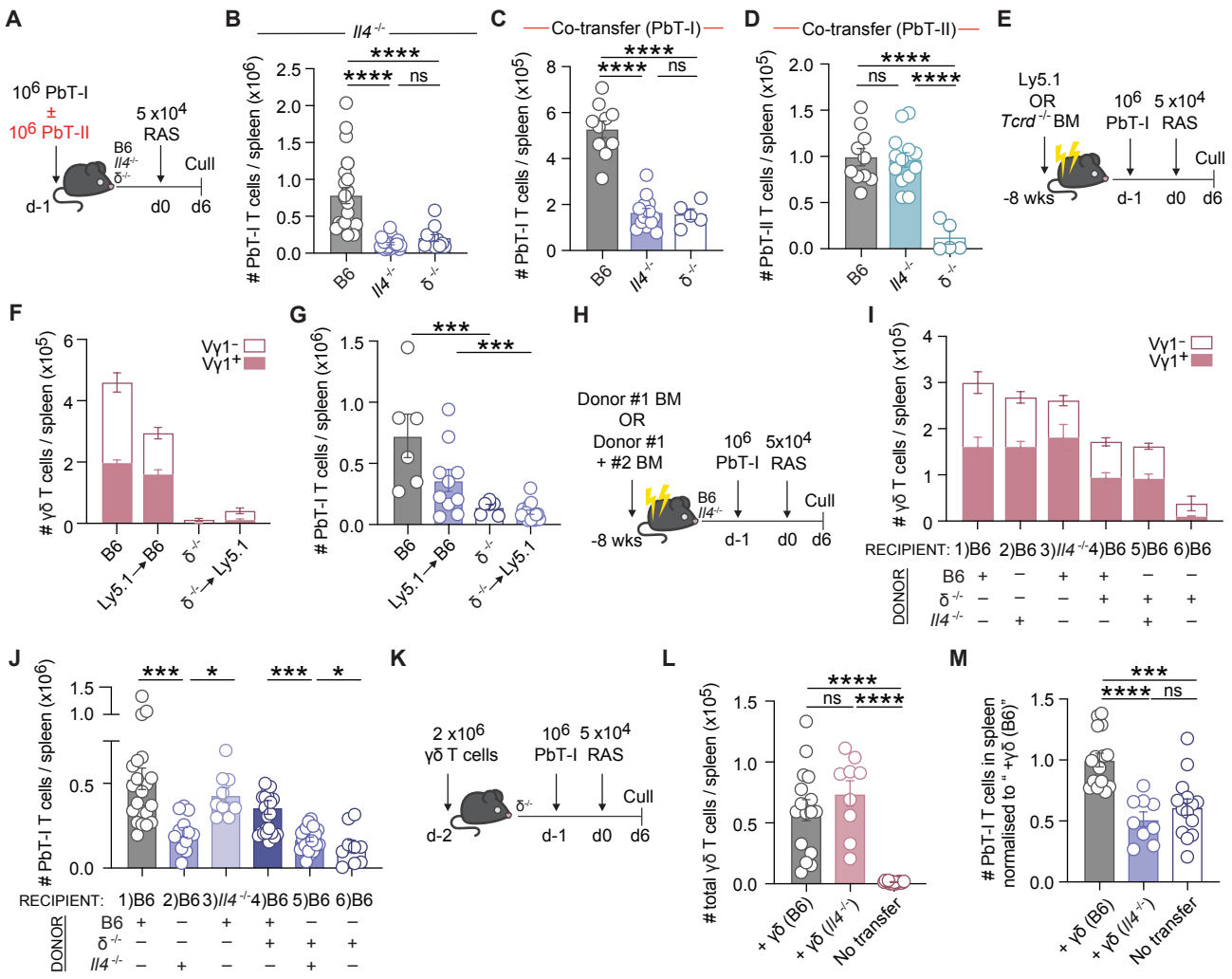
A
10^6 PbT-I
±
10^6 PbT-II
5 x10^4
RAS
B6
Il4-/-
δ-/-
Cull
d-1
d0
d6
B
Il4-/-
PbT-I T cells / spleen (x10^6)
****
****
ns
B6
Il4-/-
δ-/-
C
Co-transfer (PbT-I)
PbT-I T cells / spleen (x10^5)
****
****
ns
D
Co-transfer (PbT-II)
PbT-II T cells / spleen (x10^5)
****
ns
****
E
Ly5.1
OR
Tcrd-/- BM
10^6 PbT-I
5 x10^4 RAS
-8 wks
F
γδ T cells / spleen (x10^5)
Vγ1-
Vγ1+
Ly5.1→B6
δ-/-→Ly5.1
G
PbT-I T cells / spleen (x10^6)
***
***
H
Donor #1 BM
OR
Donor #1
+ #2 BM
10^6 PbT-I
5x10^4 RAS
I
γδ T cells / spleen (x10^5)
RECIPIENT: 1)B6 2)B6 3)Il4-/- 4)B6 5)B6 6)B6
DONOR
B6 + − + + − −
δ-/- − − − + + +
Il4-/- − + − − + −
J
PbT-I T cells / spleen (x10^6)
***
*
***
*
RECIPIENT: 1)B6 2)B6 3)Il4-/- 4)B6 5)B6 6)B6
DONOR
B6 + − + + − −
δ-/- − − − + + +
Il4-/- − + − − + −
K
2 x10^6
γδ T cells
10^6 PbT-I
5 x10^4 RAS
d-2
L
total γδ T cells / spleen (x10^5)
****
ns
****
+ γδ (B6)
+ γδ (Il4-/-)
No transfer
M
PbT-I T cells in spleen normalised to " +γδ (B6)"
***
****
ns

Figure 5

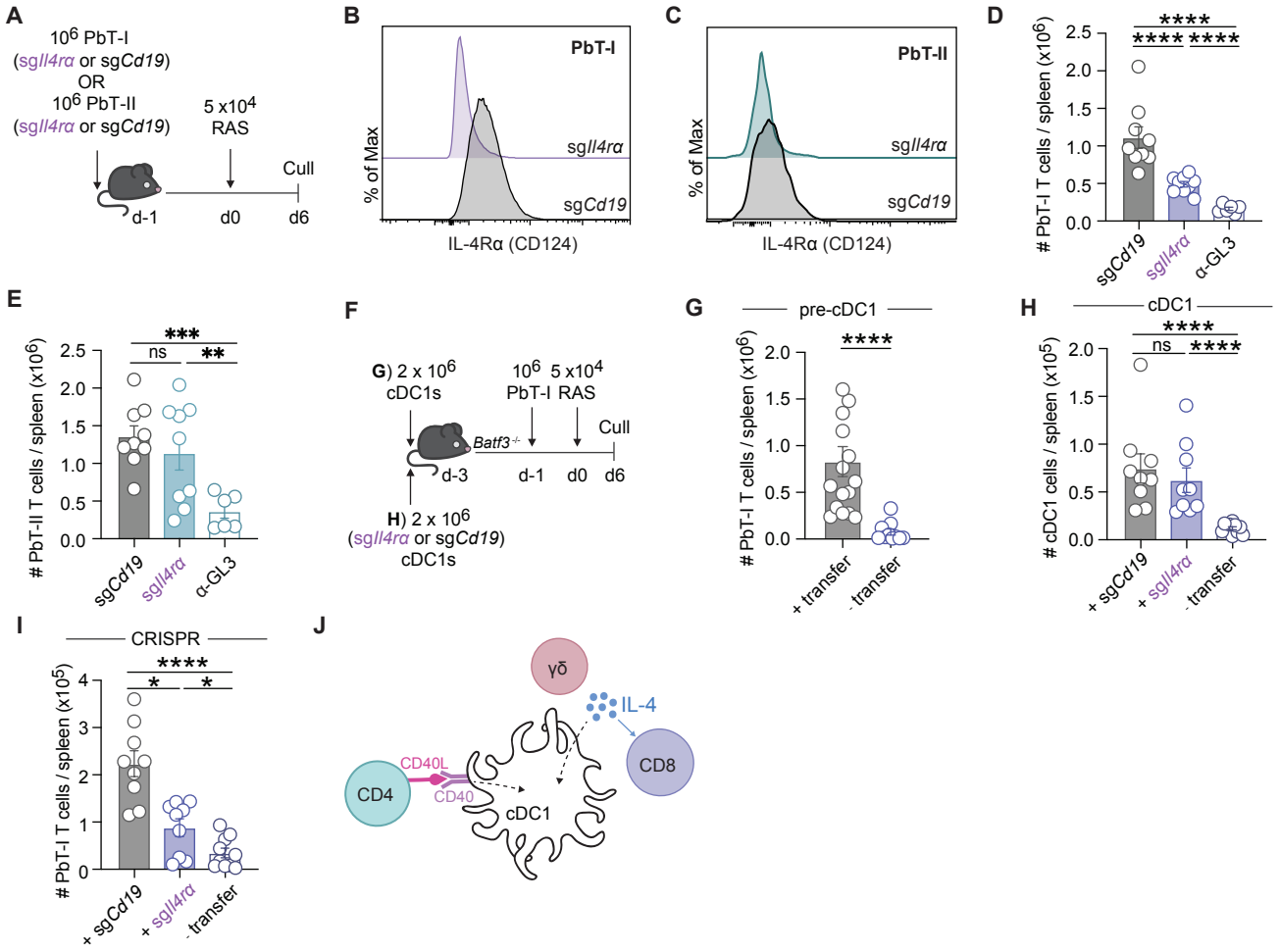
A
10^6 PbT-I
(sgIl4rα or sgCd19)
OR
10^6 PbT-II
(sgIl4rα or sgCd19)
5 x10^4
RAS
Cull
d-1
d0
d6
B
PbT-I
sgIl4rα
sgCd19
% of Max
IL-4Rα (CD124)
C
PbT-II
sgIl4rα
sgCd19
% of Max
IL-4Rα (CD124)
D
PbT-I T cells / spleen (x10^6)
sgCd19
sgIl4rα
α-GL3
E
PbT-II T cells / spleen (x10^6)
ns
sgCd19
sgIl4rα
α-GL3
F
G) 2 x 10^6
cDC1s
10^6 PbT-I
5 x10^4
RAS
Cull
Batf3-/-
d-3
d-1
d0
d6
H) 2 x 10^6
(sgIl4rα or sgCd19)
cDC1s
G
pre-cDC1
PbT-I T cells / spleen (x10^6)
+ transfer
- transfer
H
cDC1
cDC1 cells / spleen (x10^5)
ns
+ sgCd19
+ sgIl4rα
- transfer
I
CRISPR
PbT-I T cells / spleen (x10^5)
+ sgCd19
+ sgIl4rα
- transfer
J
γδ
IL-4
CD8
CD4
CD40L
CD40
cDC1

Figure 6

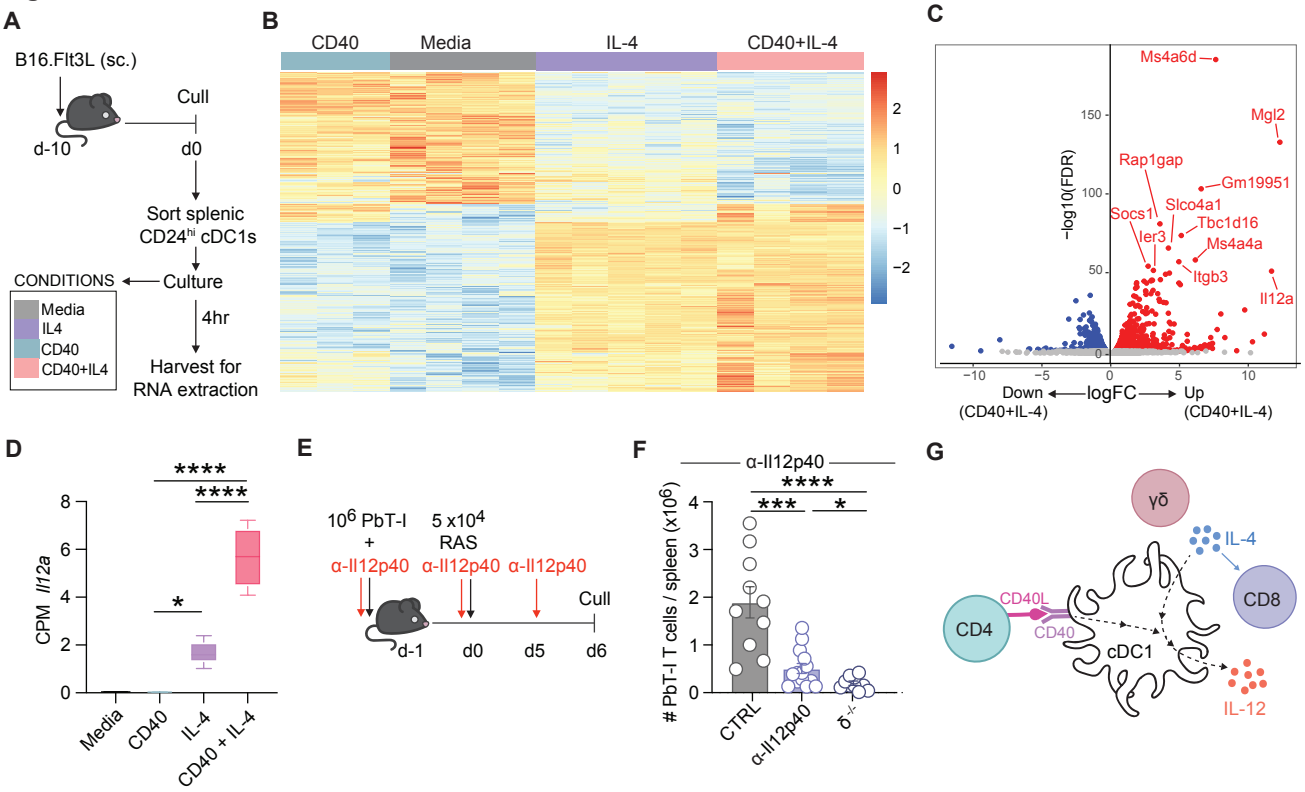
A
B16.Flt3L (sc.)
d-10
Cull
d0
Sort splenic
CD24hi cDC1s
Culture
4hr
Harvest for
RNA extraction
CONDITIONS
Media
IL4
CD40
CD40+IL4
B
CD40
Media
IL-4
CD40+IL-4
C
Ms4a6d
Mgl2
Rap1gap
Gm19951
Slco4a1
Socs1
Tbc1d16
Ier3
Ms4a4a
Itgb3
Il12a
−log10(FDR)
Down
(CD40+IL-4)
logFC
Up
(CD40+IL-4)
D
CPM Il12a
Media
CD40
IL-4
CD40 + IL-4
E
10^6 PbT-I
+
α-Il12p40
5 x10^4
RAS
α-Il12p40
α-Il12p40
Cull
d-1
d0
d5
d6
F
α-Il12p40
PbT-I T cells / spleen (x10^6)
CTRL
α-Il12p40
δ-/-
G
γδ
IL-4
CD8
CD4
CD40L
CD40
cDC1
IL-12

Figure 7

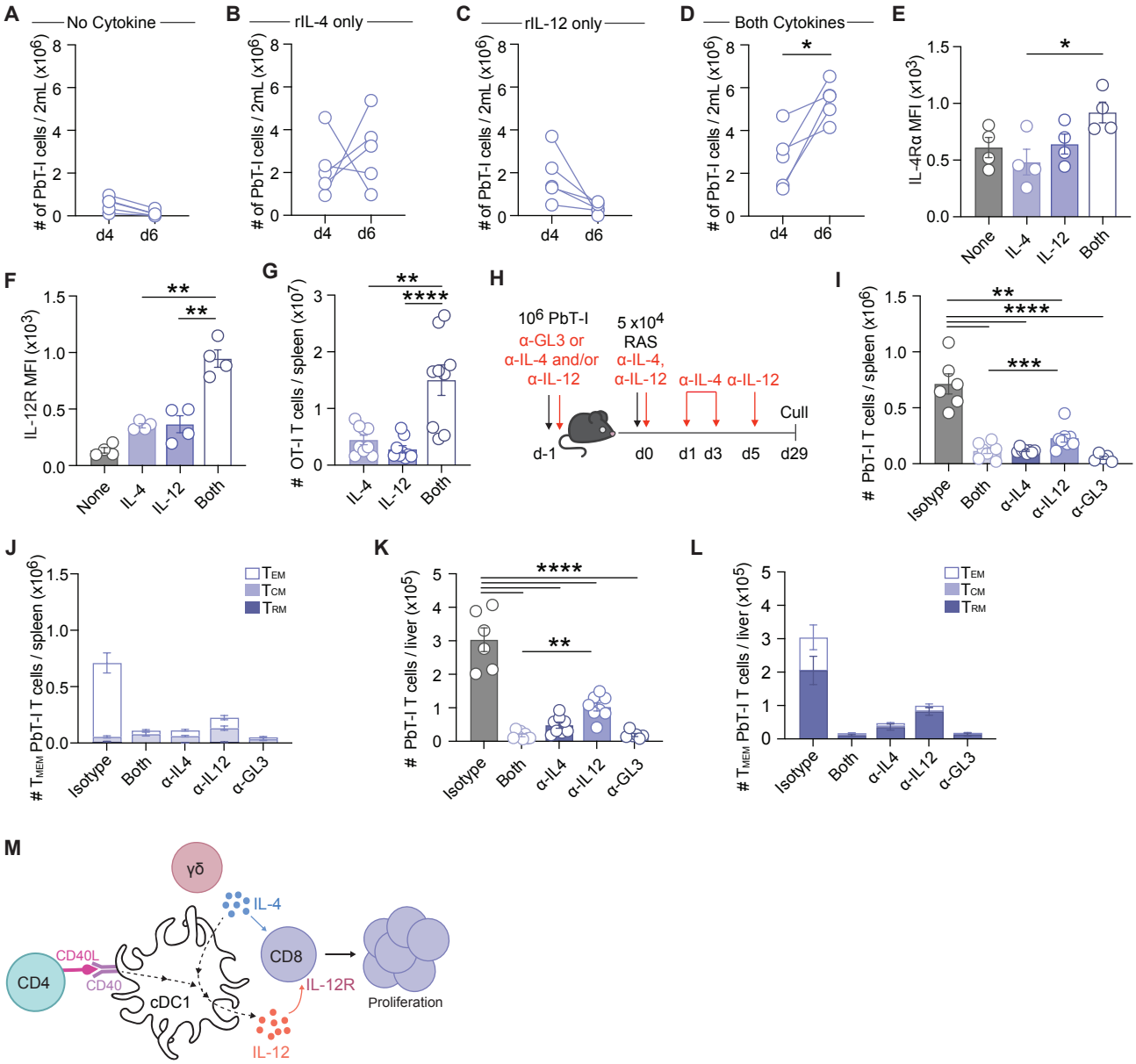
A
No Cytokine
# of PbT-I cells / 2mL (x10^6)
d4
d6
B
rIL-4 only
C
rIL-12 only
D
Both Cytokines
E
IL-4Rα MFI (x10^3)
None
IL-4
IL-12
Both
F
IL-12R MFI (x10^3)
G
OT-I T cells / spleen (x10^7)
H
10^6 PbT-I
α-GL3 or
α-IL-4 and/or
α-IL-12
5 x10^4
RAS
α-IL-4,
α-IL-12
α-IL-4 α-IL-12
Cull
d-1
d0
d1 d3
d5
d29
I
PbT-I T cells / spleen (x10^6)
Isotype
Both
α-IL4
α-IL12
α-GL3
J
TMEM PbT-I T cells / spleen (x10^6)
TEM
TCM
TRM
K
PbT-I T cells / liver (x10^5)
L
TMEM PbT-I T cells / liver (x10^5)
M
γδ
IL-4
CD8
CD4
CD40L
CD40
cDC1
IL-12R
IL-12
Proliferation